

**REAL-DATA-BASED MODELLING AND TORQUE
VECTORING ALGORITHM FOR A 4-WHEEL-DRIVE
FORMULA STUDENT VEHICLE**

Eduard Morera Torres

Director: Carlos Ocampo Martínez

June 2020



ESCOLA TÈCNICA SUPERIOR D'ENGINYERIA INDUSTRIAL DE
BARCELONA

UNIVERSITAT POLITÈCNICA DE CATALUNYA



BACHELOR'S DEGREE IN INDUSTRIAL TECHNOLOGY ENGINEERING
FINAL PROJECT

Acknowledgements

First of all, I would like to thank my family and some of my friends who have given me the support I needed during some stages of the project.

Secondly, I would like to thank the whole team of ETSEIB MotorSport. A lot of things are easier when working as a team, and the help of my teammates has been important during this project. Specially I would like to thank my Vehicle Controls department mates, this project would have been much more difficult without their help, some good ideas have came out during interesting conversations between us.

A part from my team, I would also like to thank the UPC-ETSEIB university for giving their support to projects like the Formula Student, offering the interested students the opportunity to enhance their engineering abilities thruogh an amazing experience.

Finally, I would like to thank Carlos Ocampo Martínez for his technical advising and support. We have maintained some interesting conversations and have had some fun! Also all the professionals that may have punctually given their support or collaborated in this project somehow.

Thank you all!

Abstract

In this project, a Torque Vectoring algorithm for a Formula Student vehicle with four in-wheel electrical machines is designed and tested. This algorithm includes the development of a Quasi-LPV bicycle model, the design of a Proportional-Integral yaw rate controller and the statement and solution of a Torque Distribution multi-objective optimization problem.

Data analysis and the information that can be extracted from this process is explained and discussed, as it is a fundamental procedure for each of the control modules that are going to be developed. Also a vehicle dynamics introduction is presented in order to enable a better understanding of every step that has been done throughout the project.

Finally, all the results obtained from the resultant Torque Vectoring control system are presented and discussed with its consequent conclusions.

This page is intentionally left blank.

List of Figures

1.1 Project Overlay	3
2.1 Formula Student Events Map	6
2.2 Skid-pad track regulations	8
2.3 Simple Friction Circle Diagram	9
2.4 Simple Friction Circle Diagram	9
2.5 CAT12e in Formula Student Spain, August 2019	10
2.6 CAT12d in Formula Student Spain, August 2019	10
3.1 Vehicle Reference Axis	12
3.2 Longitudinal Load Transfer Diagram	13
3.3 Lateral Load Transfer Diagram	14
3.4 Vehicle body diagram	15
3.5 Simple Friction Circle Diagram	16
3.6 Wheel Dynamics	17
3.7 Longitudinal Force vs Slip Ratio	17
3.8 Lateral Force vs Slip Angle	18
3.9 Complex Friction Circle Diagram [Mil, 1994]	19
3.10 Normalized Fx vs Slip Ratio for multiple tire loads - 3D Graph	20
3.11 Normalized Fy vs Slip Angle for multiple tire loads - 3D Graph	20
3.12 Pro-Ackermann Tire Characteristic	21
3.13 Anti-Ackermann Tire Characteristic	22
3.14 Idea vs real ICR	22
3.15 Bicycle Model Diagram	23
3.16 Understeering and Oversteering Scheme	25
3.17 Understeering, Oversteering and Neutral Plot Example	26
3.18 Ellipse 2-N	28
3.19 MTLT305D	28
3.20 Lineal Position Sensor	28
3.21 Resolver RE-15	29
3.22 Fischer Electrical machines	29
3.23 MOBILE DCU 60/60	29
3.24 Isabellenhütte IVT-MODULAR	30
3.25 DataAnalysisPro Example	30
4.1 Comparison between simple bicycle model and Quasi LPV bicycle model	36

4.2	Relative error vs Scheduling Variables Step	36
4.3	Comparison between real data and Quasi-LPV model	37
4.4	GPS Velocity during FSS Endurance	37
4.5	Comparison between IPG and Quasi-LPV model	38
5.1	Control Scheme	39
5.2	K_p Plot	43
5.3	K_i Plot	43
5.4	K_p Polynomial - $R^2=0.968$	44
5.5	K_i Polynomial - $R^2=0.968$	44
5.6	Step Response depending on operating condition	45
5.7	FFT Over Yaw Rate Signal	46
5.8	Closed Loop Bode Plot depending on operating condition	46
5.9	Feed-forward Scheme	47
5.10	Anti-Windup Scheme	47
7.1	IPG Simulation Example	54
7.2	Yaw Rate Response	57
7.3	$M_{z,TV}$ Response	58
7.4	Exitflag Value	59
7.5	F_x Response	60
7.6	Wheel Torques	61
7.7	Power Limit Behaviour	62
7.8	Skidpad Comparison	63

List of Tables

2.1	Punctuation Table	9
5.1	K_p Values for multiple operating conditions	42
5.2	K_i Values for multiple operating conditions	42
5.3	Polynomial constants	43
7.1	Influence of the prioritized objectives	55
7.2	Skidpad Comparison	63
8.1	Costs table for involved tasks	65
8.2	Costs table for involved resources	65

Nomenclature

Vehicle Variables

m	Vehicle mass [kg]
J_v	Vehicle Yaw Inertia [kg m^2]
CoG	Vehicle Center of gravity [kg m^2]
h_{CoG}	Vehicle Center of gravity height [m]
L	Vehicle wheelbase [m]
lf	Vehicle distance from CoG to front axle [m]
lr	Vehicle distance from CoG to rear axle [m]
tf	Vehicle front track width [kg]
tr	Vehicle rear track width [kg]
gr	Vehicle transmission ratio [-]
R_ω	Wheel Radius [kg m^2]
J_ω	Wheel Inertia [kg m^2]

Kinematic & Dynamic Variables

g	Gravity [m/s^2]
v_x	Vehicle Longitudinal Velocity [m/s]
v_y	Vehicle Lateral Velocity [m/s]
$\dot{\psi}$	Vehicle Yaw Rate [rad/s]
a_x	Vehicle Longitudinal Acceleration [m/s^2]
a_y	Vehicle Lateral Acceleration [m/s^2]
$\ddot{\psi}$	Vehicle Yaw Rate [rad/s]
δ	Driver Steering Angle [rad]

δ_ω	Steering Angle of a determined wheel [rad/s]
$\ddot{\psi}$	Vehicle Yaw Rate [rad/s]
$W_{s,i}$	Static Load for a determined tire [N]
W_{lot}	Longitudinal transferred load [N]
M_z	Moment around the Z axis of the vehicle [Nm]
M_z	Total moment around the Z axis of the vehicle [Nm]
$M_{z,Fy}$	Moment around the Z axis of the vehicle due to lateral forces [Nm]
$F_{x,i}$	Longitudinal force of a determined tire [N]
$v_{x,i}$	Longitudinal velocity of a determined tire [m/s]
$v_{y,i}$	Lateral velocity of a determined tire [m/s]
α_i	Slip angle of a determined tire [rad]
σ	Slip ratio [-]
$\dot{\omega}_\omega$	Angular acceleration of a determined wheel [rad/s ²]
β	Slip angle of the vehicle at the <i>CoG</i> [rad]
α_F	Slip angle of the front axle [rad]
α_r	Slip angle of the rear axle [rad]
C_f	Cornering stiffness of the front axle [N/rad]
C_r	Cornering stiffness of the rear axle [N/rad]
ω_ω	Angular velocity of a determined wheel [rad/s]

Control Variables

$M_{z,TV}$	Moment around the Z axis due to the Torque Vectoring [Nm]
Γ_i	Commanded torque to each wheel [Nm]
K_{pi}	Proportional variable of the PI controller [Nm/rad]
K_i	Integral variable of the PI controller [Nm/rad]
α_m	Priority variable for each of the TD objectives [-]
J_m	Objectives of the TD problem [-]
$F_{x,min}$	Lower limit for the F_x variable in the TD problem [N]
$F_{x,max}$	Upper limit for the F_x variable in the TD problem [N]

$M_{z,min}$ Lower limit for the F_x variable in the TD problem [Nm]

$M_{z,max}$ Lower limit for the F_x variable in the TD problem [Nm]

P_{max} Upper limit for the developed power in the TD problem [Nm]

F_x^{ref} Desired value for the F_x in the TD problem [N]

M_z^{ref} Desired value for the M_z in the TD problem [Nm]

t_s Simulation time [s]

V_b Battery voltage [V]

I_b Intensity of the battery [A]]

Acronyms

ECU Electronic Control Unit

GPS Global Positioning System

IMU Inertial Measurement Unit

LQR Linear Quadratic Regulator

PID Proportional-Integral-Derivative

TD Torque Distribution

TV Torque Vectoring

Contents

Acknowledgements	i
Abstract	ii
List of Figures	v
List of Tables	vi
Nomenclature	vii
Acronyms	x
1 Introduction	1
1.1 Motivation	1
1.2 State of the art	1
1.3 Objectives	2
1.4 Project Overlay	3
2 Formula Student	5
2.1 Brief Introduction to Formula Student	5
2.2 Formula Student Event Organization	5
2.3 ETSEIB MotorSport - Driverless UPC	9
3 Vehicle Dynamics	11
3.1 Introduction to Vehicle Dynamics	11
3.2 Vehicle Space Movements	12
3.3 Longitudinal and Lateral Load Transfer	13
3.3.1 Longitudinal Load Transfer	13
3.3.2 Lateral Load Transfer	14
3.4 Tires	14
3.4.1 Friction Circle	15
3.4.2 Slip Ratio - Longitudinal Force	16
3.4.3 Slip Angle - Lateral Force	18
3.4.4 Vertical Force	19
3.4.5 Ackermann Steering Geometry	21
3.5 Three-Degrees-of-Freedom Bicycle Model	23
3.6 Vehicle Behaviour/Sensitivity	25

3.7	Vehicle Data Analysis	27
3.7.1	Data Acquisition	27
3.7.2	Sensors and actuators	27
3.8	Data Analysis Software	30
3.9	Summary	31
4	Yaw Rate Control-Oriented Dynamic Model	32
4.1	Problem Statement	32
4.2	Linear Parameter Varying Model	33
4.2.1	LPV Model Types	33
4.2.2	LTI vs LPV	34
4.2.3	LTV vs LPV	34
4.3	Quasi-LPV Bicycle Model	34
4.4	Summary	38
5	Yaw Rate Control Design	39
5.1	General Control Scheme	39
5.2	Yaw Rate Reference Signal	39
5.3	Yaw Rate Controller Design	41
5.4	Yaw Rate Controller Response	45
5.5	Feed-Forward Component	46
5.6	Anti-windup Component	47
5.7	Summary	48
6	Torque Distribution Problem	49
6.1	Introduction to Torque Vectoring	49
6.2	Torque Distribution Control-Oriented Model	50
6.3	Torque Distribution Optimization Problem	50
6.4	Summary	53
7	Torque Vectoring Simulation and Results	54
7.1	Introduction to simulation and results	54
7.2	Torque Distribution	55
7.3	Analysis of the vehicle behaviour	57
7.3.1	Yaw Rate Controller	57
7.3.2	Desired M_z vs Developed M_z	58
7.3.3	Desired F_x vs Developed F_x	59
7.3.4	Torques	60
7.3.5	Power Limitation	61
7.3.6	Torque Vectoring Active vs Torque Vectoring Disabled (25% Distribution)	62
7.4	Summary	63
8	Economical Analysis	65
9	Environmental impact	66
10	Conclusions & Further Work	68

References

71

Chapter 1

Introduction

1.1 Motivation

Formula Student (FS) is a great ante-room for a lot of students all around the world who are interested in getting in touch with the automotive industry, or even many other engineering fields. This competition is defined for the eager to learn about vanguard technologies and its implementation into formula-type prototypes, whose ongoing evolution, which follows the automotive market trends, leads to quite challenging problems for all the participants involved each season.

ETSEIB MotorSport is a team participating in the FS competition since 2007. Starting with a vehicle powered by an internal combustion engine motor, the team made a step-forward to an electric vehicle in 2011. Until 2017, the electric prototype was driven by a single motor and in 2018, a project to build a four wheel-driven car was planned. With the decision of re-designing the whole power-train assembly, the necessity of a control system to regulate the power distribution between the four vehicle actuators appeared. Such a control algorithm is called Torque Vectoring (TV).

The inclusion of TV technology offers the possibility to modify and adapt the behaviour of a vehicle to many different conditions and situations (always under dynamic limitations), and some of the improvements it allows to implement are in terms of performance, energy management or safety. The possibility to deepen into vehicle dynamics knowledge together with the design and implementation of a TV algorithm is quite challenging and entails the bases of this project.

1.2 State of the art

Over the last 15 years, there has been a high level of inclusion of electrical components into the power-train of vehicles. In a lot of vehicle models, those electrical components work together with internal combustion engines and the mechanical elements this kind of power-trains entail to distribute its power. Besides that, another branch of the automotive industry has been considerably increasing, which is the fully-electric mobility. Either talking about an only electric or a hybrid power-train vehicle, both have in common that a power distribution

algorithm must be implemented to manage and control the motors or electrical machines, so a TV algorithm to fulfill each of the demands of each type of power-train needs to be designed.

Regarding the concrete case that this project is focused on, the power-train is configured by four in-wheel motors, one mounted to each of the wheel assemblies, whose control algorithm claims the necessity of the same modules that any other kind of vehicle with an implemented TV needs. Such control modules are a yaw rate controller to determine the extra moment around the Z axis of the vehicle that is needed to fulfill a yaw rate request, and the solution of a Torque Distribution (TD) problem to distribute the power over the actuators.

Regarding the yaw rate controller, the most commonly studied approaches are the use of a Proportional-Integral-Derivative (PID) controller type [Mikle and Bat'a, 2019], Linear Quadratic Regulator (LQR) [Antunes et al., 2019] or H_∞ methods [Doumiati et al., 2010]. Together with the design of the controller, the development of a control-oriented model is essential. A quite common approach is the use of an automotive bicycle model depending on the velocity [Han, 2015], which some studies have improved by the inclusion of a piece-wise tire model [Gang Liu et al., 2013].

Regarding the TD problem, there are common approaches that base its power distribution on dividing it over each of the side of the vehicle (corresponding to the left and right side motors), which may be suitable in the case of a two power-train actuators [Antunes et al., 2019], but needs a further distribution over front and rear wheels of each side based on vertical loads if there are also motors assembled into the front axle [Trunas Bruguera, 2019] not considering slip angles. There are also approaches focused on the reduction of tire power losses [Kevin Ghezzi, 2017] and, when talking about hybrid vehicles, the approach has to include the modelling of all the mechanical components [Velazquez Alcantar and Assadian, 2019].

1.3 Objectives

The overall purpose of this project is to design a TV control system for a Formula Student prototype, whose power-train is composed of four in-wheel independent motors. This overall objective can be decomposed into the following specific objectives:

- Determine of a yaw rate control-oriented model based on real data logged from the previous season vehicle. In this case, the selected approach is a self-designed bicycle model which includes the sensitivity of the vehicle in terms of understeering and oversteering. This objective requires an extended data analysis and the correspondent selection of the necessary data information to be included into the model.
- Design a yaw rate controller that ensures a suitable reference generation for one of the most important control signals of the algorithm: the extra moment around the Z axis of the vehicle that the actuators must develop ($M_{z,TV}$).
- State and solve a TD multi-objective optimization problem with its correspondent constraints to improve the overall performance of a vehicle.

- Suitably join the yaw rate controller together with the TD problem. To do so, it is purposed to include this control modules into a Simulink model inside the simulation software IPG-CarMaker.
- Implement the designed algorithm into the main Electronic Central Unit (ECU) of the CAT13e, the 2020-2021 vehicle of ETSEIB MotorSport, and the analysis of its behaviour into the real prototype. Regarding this objective, it has not been possible to carry through due to the actual extraordinary situation that the world is going through. The submission of this project is done in June, 2020, and during the last three months, people have had to stay at home because of a global pandemic, which has also forbid doing any work that could not be done from home such as the one regarding this point.

1.4 Project Overlay

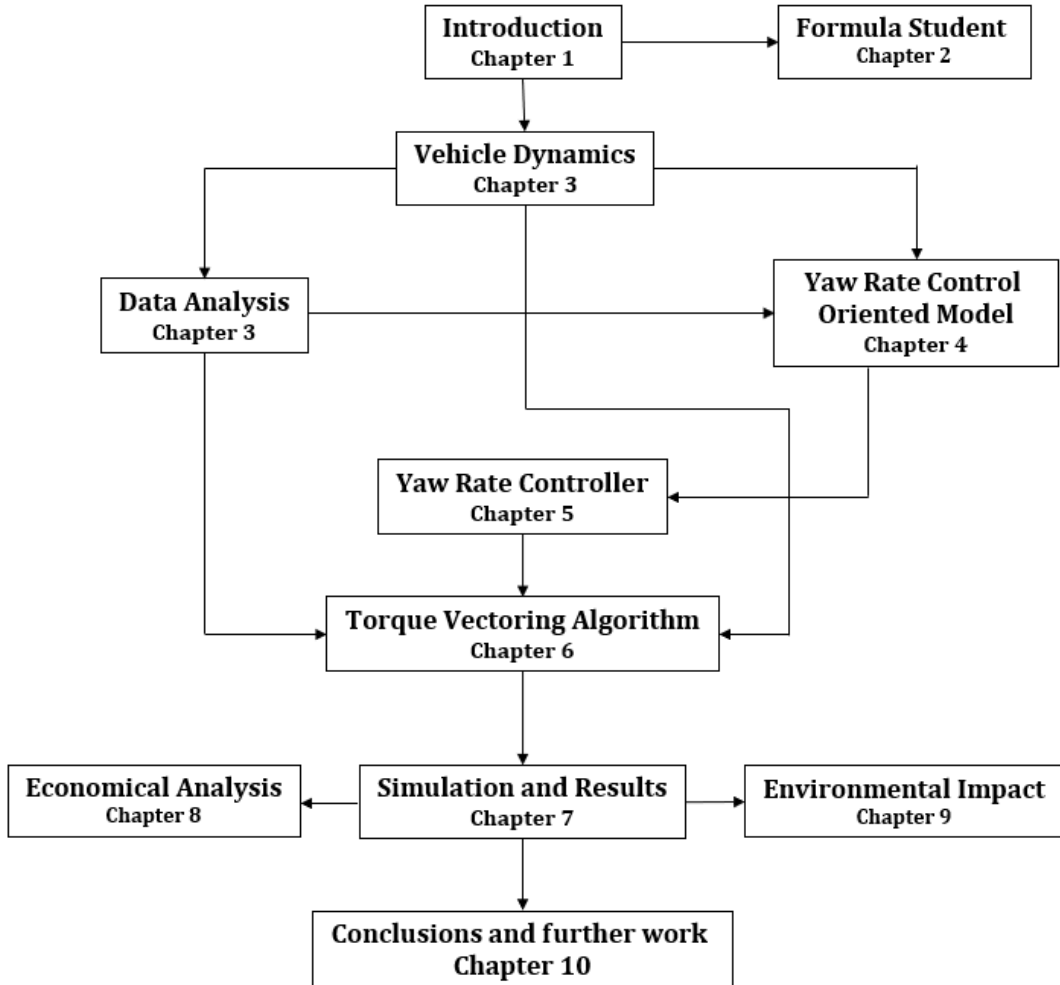


Figure 1.1: Project Overlay

In this section, an scheme (Figure 1.1) is presented to facilitate the understanding of the organization of this project. Together with this figure, an introduction of all the chapters are presented as follows:

- Chapter 2 - Formula Student

In Chapter 2, a brief introduction to the Formula Student competition is presented in order to set a background for this project. Apart from that, also a presentation of the team ETSEIB MotorSport is outlined.

- Chapter 3 - Vehicle Dynamics

In Chapter 3, an introduction to vehicle dynamics concepts that are going to be used in the subsequent chapters are presented and explained, together with the support of data obtained from the CAT12e, the vehicle of ETSEIB MotorSport for the 2018-2019 Formula Student season.

- Chapter 4 - Yaw Rate Control-Oriented Dynamic Model

In Chapter 4, a control-oriented model, based on real data, is developed. This model is crucial for the design of the control components of the TV.

- Chapter 5 - Yaw Rate Control Design

In Chapter 5, a PID-type controller is developed and the analysis of its response is presented. This controller is designed by using the control-oriented model presented in Chapter 4.

- Chapter 6 - Torque Distribution Problem

In Chapter 6, the TD multi-objective optimization problem is defined together with a detailed explanation of all its objectives and constraints to obtain an optimal distribution of the power through the four actuators of the vehicle.

- Chapter 7 - TV Simulation and Results

In Chapter 7, the results of the simulation of all the control components assembled are presented and discussed, determining the benefits of the inclusion of a TV system.

- Chapter 8 - Economical Analysis

In Chapter 8, an unblock of the economical costs of this project is presented, from both which would be the cost for carrying this project out of a students-environment, and the real cost this project has meant.

- Chapter 9 - Environmental Impact

In Chapter 9, a brief explanation about the benefits that can mean the implementation of a TV system over a vehicle are presented.

- Chapter 10 - Conclusions & Further Work

In Chapter 10, there is a detailed explanation about the main contributions that the results of this project delivers to the ETSEIB MotorSport team, together with a summary of the tasks that have been performed and other tasks which may be further done.

Chapter 2

Formula Student

2.1 Brief Introduction to Formula Student

Formula Student is an engineering competition which gathers universities all over the world with the objective of enhancing the learning process of all the students participating in it. It is mainly related to the automotive industry, but it covers multiple aspects of engineering itself.

It was created under the name of Formula SAE (FSAE) in the United States in 1980 by Ron Matthews, Mike Best, Robert Edwards and John Tellkamp backed up by the Society of Automotive Engineers (SAE). Until 1998, the competition was only held in the United States, but after a participation of English teams which attended, the organization decided to organize a second competition in the United Kingdom, under the management of the Institution of Mechanical Engineers (IMechE) in partnership with SAE. From that, teams all over the world were created by multiple universities which started to join the competition.

It was in 2010 when SAE International recognized three more competitions official ones: Formula Student Germany, Formula Student Austria and Formula Student Japan. Specifically in Europe, it was created under the name of Formula Student, with the regulations established in Germany. At that point, an electric class was introduced, giving the teams the opportunity to choose between combustion or electric motors, and it was in 2017 when the driver-less class was finally introduced.

Nowadays there are more than 700 teams all over the world joining this competition which has also grown in number of events with a total of 17 (Figure 2.1) held in multiple countries.

2.2 Formula Student Event Organization

There is a common distribution between all the Formula Student and FSAE events, which is the internal organization of all the sub-events explained above.



Figure 2.1: Formula Student Events Map

Quiz

This is a previous task for all teams desiring to participate in Formula Student events as there are limited slots. *Quizzes* are tests organized during a day which all the teams do at the same time. Every competition does its own *quiz* with their own style and the teams with higher marks, together with less time needed are the ones that take the slot.

Technical Inspection

As mentioned before, the competition has its own rules, which mainly determine what a Formula Student car needs to be safe enough to be driven. To determine if any car is rules compliant, every team has to pass some tests carried out by the competition technical inspectors:

- **Pre-Inspection**

It is a simple revision to bear out that all the driver equipment presented by a team is rules compliant and in a good state together with the tires and rims and the fire extinguishers.

- **Electrical Inspection**

The main objective of this part is to determine if a car is electrically safe and rules compliant with all the electrical points such as the shut-down security circuit, all the electrical cables or the security firewalls.

- **Accumulator Inspection**

The suitable state of the battery is analyzed together with its security items. That is done together with a revision of the battery charger.

- **Mechanical Inspection**

The main objective of this part is to determine if a car is mechanically safe and rules compliant. Components such as the chassis, wheel assembly, suspension or refrigeration system, between others, together with all the junctions are revised.

- **Tilt Test**

The objective of this test is to determine if the car can handle a lateral acceleration corresponding to 1.7g. To do so, the car is laid on a platform which raises from one side taking the car until 60° with the floor horizontal plane.

- **Rain Test**

The objective of this test is to determine if all the electrical components are well protected from water and, apart from that, to determine if the high voltage and low voltage circuits are correctly isolated. To do so, the car is sprayed with water during 120s and left 120s more without being sprayed to see if the isolating sensor calculates a resistance below 250 Ω/V. If it does not do so, the test is passed.

- **Brake Test**

The main objective of this test is to determine if a car is able to block the wheels while braking and if it is stable during that maneuver. To validate a suitable braking, the car accelerates in a straight line, brakes at a determined distance and the competition staff determine if the maneuver fulfilled the requirements to pass.

Static Events

- **Business Plan Presentation**

The team has to present a business plan in which the Formula Student prototype has to be included, showing that it can be profitable. A team of judges are going to value it.

- **Cost and Manufacturing**

All the materials and processes needed to build the car have to be exposed together with its corresponding costs. A team of technical judges are going to value it and ask for any doubts or how possible modifications would affect the final cost.

- **Design**

The decisions taken until the final state of the components in the car have to be presented. The exposing members have to explain to a group of technical judges all the considered options during the design process and what they know about the prototype.

Dynamic Events

- **Acceleration**

The car has to run over a 75m long straight as fast as possible. Traction and power



controls are crucial, as the aim is to do it as fast as possible without exceeding the limit power of 80kW determined by the rules.

- **Skid-pad**

The car has to turn twice right and twice left (in this order) around the track presented in Figure 2.2. This event is taken to analyze the stability while cornering and also while making a fast direction change.

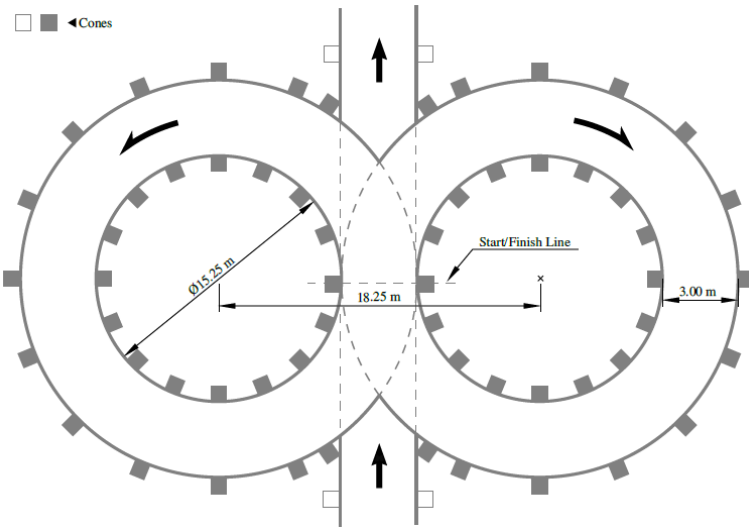


Figure 2.2: Skid-pad track regulations

- **Autocross**

The aim is to make the fastest possible lap around a circuit determined by each competition event. The total length of the track tends to be around 1km and it has to fulfill some limitations established in the regulations such as minimum turning radius or track width.

- **Endurance**

The main objective is to finish a 22km run around the same (or similar) circuit of the Autocross event. This is the toughest test as it evaluates the reliability of all the components of the car and the capacity of maintaining the pace. There are several cars on the track at the same time, although wheel-to-wheel running is not allowed. For that reason there are zones where the car that is going to be passed has to go through to allow the car behind it to pass in case it is faster.

- **Efficiency**

This is a test inside the Endurance itself which evaluates the efficiency of the cars in terms of energy usage.

At the beginning and at the end of every event there is a *pre* and *post* scrutineering. At the *pre-inspection*, the judges determine if a car is still rules compliant and confirm that non-allowed changes have been done since the inspections. On the other hand, at the

post-scrutineering the judges analyze that all the systems are in good state and if there have been any reliability problem, which would suppose a disqualification of a run or of that test itself.

Punctuation

There is a maximum of 1000 points which teams can obtain depending on their performance during all the events. This punctuation is presented in Table 2.1.

Table 2.1: Punctuation Table

Event	Type of event	Punctuation
Acceleration	Dynamic Event	75
Autocross	Dynamic Event	75
Business Plan	Static Event	75
Skid-pad	Dynamic Event	100
Efficiency	Dynamic Event	100
Cost and Manufacturing	Static Event	100
Design	Static Event	150
Endurance	Dynamic Event	325

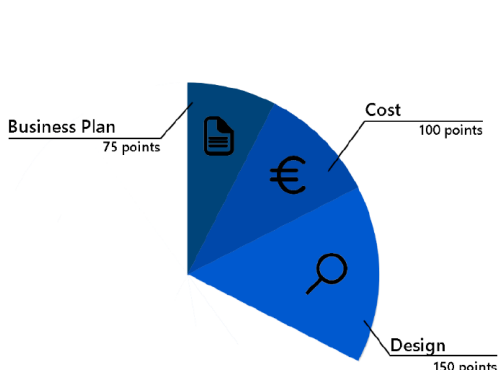


Figure 2.3: Simple Friction Circle Diagram

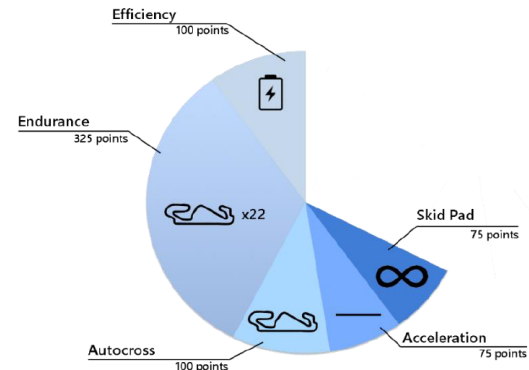


Figure 2.4: Simple Friction Circle Diagram

2.3 ETSEIB MotorSport - Driverless UPC

The team was created in 2007, when a group of students decided to join the competition by creating the first prototype with a combustion motor, the CAT01. This was the base that evolved until CAT04, the first car that took the team to a podium of a dynamic event in the Skid-pad test.

The automotive industry started to get higher interest in the electrical mobility, and the natural decision for the team was to follow that change. After four years competing in the combustion category, in 2011 the team decided to built its first full-electric vehicle, the



CAT05e, which was presented in 2012. This prototype evolved until CAT11e. Modifications an improvements had been done over all aspects of the car, and at that point, in 2018, the team decided to change its concept by extracting the motor used in CAT11e and assembling a complete new power-train based on four electrical machines, one assembled at each wheel with all the technical modifications it carries, from the chassis to the control of the electrical machines. In fact, at that point was when the *Vehicle Controls Department* was created by the necessity of implementing a TV algorithm.



Figure 2.5: CAT12e in Formula Student Spain, August 2019

Together with this changes, the team also decided to join the Driver-less category by creating its first driver-less prototype. The main objective was to implement new sensors and cameras reusing parts from older electric vehicles of the team and design the control algorithms to plan the route that the has to follow and control the actuators the right way to follow it.



Figure 2.6: CAT12d in Formula Student Spain, August 2019

Nowadays, the team is continuing the evolution of the prototypes started last season, both electric and driver-less one. The future objective it to be able to assemble the best of both vehicles to crate an autonomous vehicle with four in-wheel motors.

Chapter 3

Vehicle Dynamics

3.1 Introduction to Vehicle Dynamics

Vehicle dynamics are defined as the motion of a vehicle due to the inputs for which it is affected, which can mostly come from three different sources:

- **Driver:**

The driver is the main responsible to extract the highest performance out of a car. It is the person in charge to manage the steering and the accelerator and braking pedals together with finding the vehicle dynamic limitations. In this particular case, it is important to notice that the accelerator pedal works as a *torque encoder*, sending a desired torque reference, and the braking pedal is divided in two parts, also a *torque encoder* one (as the car is able to regenerate) and one which actuates directly to the hydraulic braking system.

- **Track:**

The car is directly affected by the asphalt of the track below it. Every asphalt has its own characteristics, more precisely, its own friction coefficient, the variable that is going to have more effect over the behaviour of the tires and, consequently, over the vehicle.

- **Environment:**

No matter the nature of the vehicle, aerodynamics is an important factor influencing the energy losses due to the *drag-force* (which is quadratically related to the relative velocity between the airflow and the body) and the extra weight it generates over the car due to the *down-force*. In racing cars, both variables are really important to take into account. As the cars are designed to be as light as possible, the down-force gives an extra weight which, well-treated, can be identified as more tire grip. On the other hand, the car must be as fast as possible in a straight sector, so drag-force needs to be minimized.

It is important to know which variables can externally affect a vehicle. However, more important than that fact, it is crucial to know the internal response of the car and how it is going to behave in any working condition; how it can move and how it is going to react to those external inputs. Some suitable references about vehicle dynamics are [Mil, 1994] and [Rac, 2014].

3.2 Vehicle Space Movements

As kinematic and dynamic variables such as velocities, accelerations and forces are the center points of analysis in a vehicle, it is important to have a well-defined reference fixed to the body of the vehicle. In the automotive sector, it is commonly used the reference axis showed in Figure 3.1, which is the same that has been used in this project. A car itself has three important movements in space: yaw, pitch and roll, one affecting each axis.

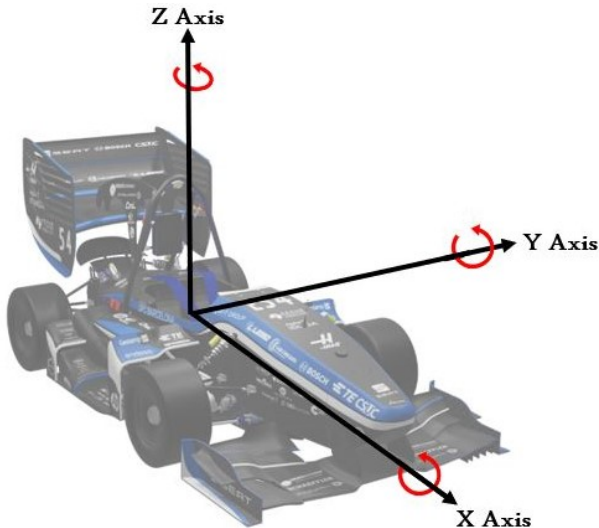


Figure 3.1: Vehicle Reference Axis

- **Yaw:**

Yaw is the movement around the *Z Axis* (Figure 3.1). However, it is important to introduce here the *yaw rate*, which is defined as the angular velocity of the car around that vertical axis, which is the result of the kinetic momentum due to external forces. It has a very high importance as it is the referred movement when talking about vehicle while turning, the main focus of this project.

- **Pitch:**

Pitch is the movement of the front and rear parts of the vehicle around the *Y Axis* (Figure 3.1), resulting from both accelerating and braking forces. Its importance lies on the fact that it directly affects the longitudinal load transfer (Section 3.3.1) during those states and the behaviour of the aerodynamic devices.

- **Roll:**

Roll is the movement of the left and right parts of the vehicle around the *X Axis* (Figure 3.1), resulting from lateral accelerations while cornering. Its importance lies on the fact that it directly affects lateral load transfer (Section 3.3.2) while turning and also the behaviour of aerodynamic devices.

3.3 Longitudinal and Lateral Load Transfer

A car has a self weight distribution determined by all the components that are assembled in itself, which determines its center of gravity. That means that in static state, the weight may not be equally distributed among all the tires, and each one has its own static load (W_s). A car tends to be symmetric in the vertical longitudinal plain, however, it is not that way in the vertical transversal one, so here is where weight distribution matters. Taking the presented consideration into account, load transfer is an important variable to consider especially in Formula-type vehicles, as it modifies the *pre-established* weight distribution in every single movement of the car, which is a crucial aspect influencing the car behaviour, as the vertical force in each tire directly affects the lateral and longitudinal forces it can handle as explained in Section (3.4).

3.3.1 Longitudinal Load Transfer

Longitudinal load transfer is the result of accelerating and braking forces. It depends on the longitudinal acceleration value, together with the height of the center of gravity and the distance between that virtual point and the front and rear axes. It is possible to find the presented mechanics relation using the free-body diagram in Figure 3.2.

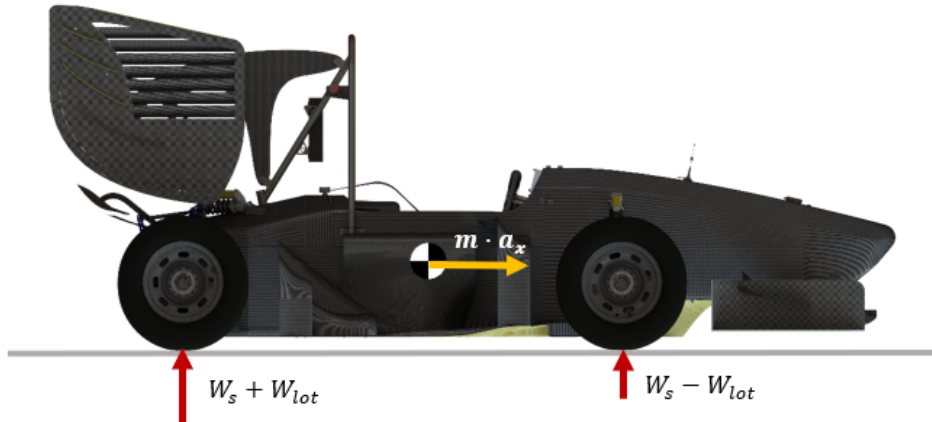


Figure 3.2: Longitudinal Load Transfer Diagram

By applying the movement quantity conservation and the kinetic momentum theorem, it is possible to determine the value of the load transfer depending on the acceleration as follows:

$$W_{lot} = \frac{h_{CoG} m a_x}{L}, \quad (3.1)$$

where h_{CoG} [m] is the height of the center of gravity, m [kg] is the mass of the vehicle (together with the mass of the driver), a_x [m/s^2] is the longitudinal acceleration and L [m] is the wheelbase.

3.3.2 Lateral Load Transfer

Longitudinal load transfer is the result of lateral forces. It depends on the lateral acceleration value, together with the height of the center of gravity and the distance between this *virtual point* and the contact surface tire-track at each side of the vehicle. It is possible to find that relation using the free-body diagram in Figure 3.3.

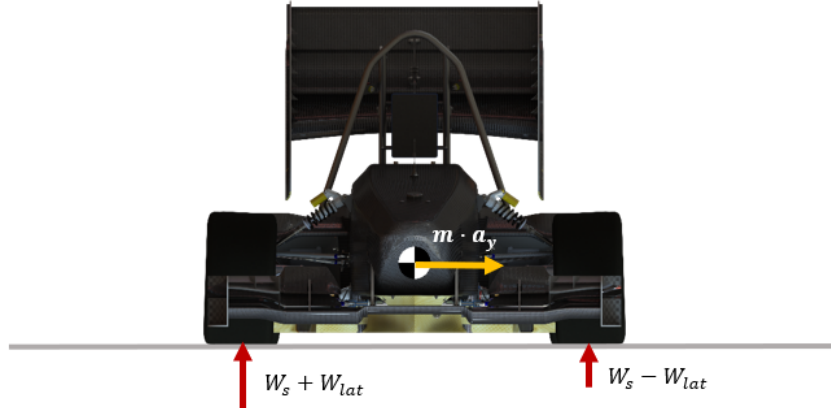


Figure 3.3: Lateral Load Transfer Diagram

By applying the movement quantity conservation and the kinetic momentum theorem, it is possible to determine the value of the load transfer depending on the acceleration as follows:

$$W_{lat} = \frac{h_{CoG} m a_y}{l_\tau}, \quad (3.2)$$

where a_y [m/s²] is the longitudinal acceleration and l_τ [m] is the length of the track of the axle, being it be the front ($\tau = f$) or the rear ($\tau = r$) respectively.

3.4 Tires

"Driving a car as fast as possible (in a race) is all about maintaining the highest possible acceleration level in the appropriate direction."

— Peter G.Wright, Team Lotus Technical Director

Thinking about that just for a moment, it is straightforward to realize that the only part of the car in contact with the ground are the tires. Having a suitable knowledge about their behaviour and limits is essential to take the most out of a car. There are many variables that influence their performance, however, the ones that are measurable in this project are which are going to be presented below in Sections 3.4.2, 3.4.3 and 3.4.4.

A free-body diagram is represented in Figure 3.4, where all the forces that a vehicle can receive through the tires are exposed, together with the velocity components and slip angles

corresponding each tire. This diagram is introduced here as it is important for further explanations of the forces considered from the tire in the following sections. Moreover, it is going to be used again in Section 6.3 as the equations that govern the TD problem are extracted from this same diagram.

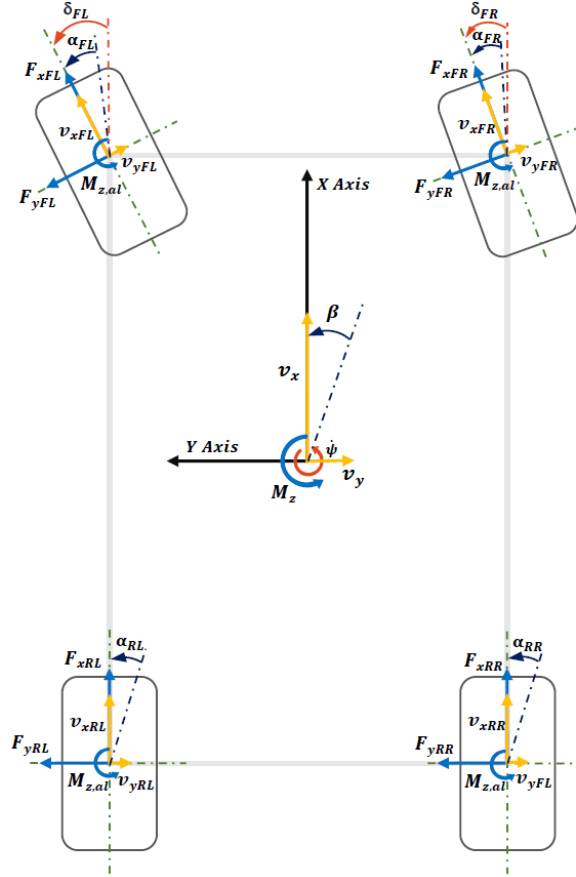


Figure 3.4: Vehicle body diagram

In Figure 3.4, $F_{x,i}$ [N] are the longitudinal forces corresponding to each tire, $F_{y,i}$ [N] are the lateral forces, $v_{x,i}$ [m/s] are the longitudinal tire velocities in respect to their own reference axis, $v_{y,i}$ [m/s] are the longitudinal tire velocities in respect to their own reference axis, α_i [rad] are the slip angles for each tire and δ_i [rad] are the steering angles corresponding to the front wheels, which may be different due to the Ackermann steering geometry (Section 3.4.5).

3.4.1 Friction Circle

The friction circle of a tire is defined as its force-producing limits in certain operating conditions. There are several variables that are going to determine those limitations: the pressure and temperature of the tire, the friction coefficient between the tire and the track, slip ratio and slip angle (the last three ones are explained in more detail in Sections 3.4.4, 3.4.2 and 3.4.3, respectively) and also the vertical tire load [Mil, 1994].

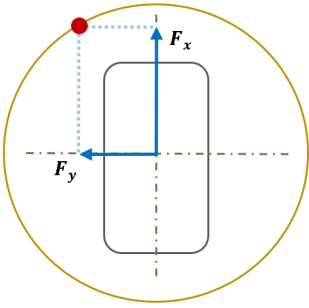


Figure 3.5: Simple Friction Circle Diagram

The aim of the simplified friction circle represented above (Figure 3.5) is to show how F_x and F_y are directly related and limited by each other depending on the working state of the tire. For a determined F_x , there is a limited available F_y and the other way round. That explains, for example, why experienced drivers do not demand much torque during curves or why they do not turn much while hard braking, as the available force in the optimal direction would be reduced. This concept can also be extracted from the following equations:

$$F_t = \sqrt{F_x^2 + F_y^2}, \quad (3.3a)$$

$$F_\chi = \mu F_z, \quad (3.3b)$$

$$F_\gamma = F_\chi - F_t, \quad (3.3c)$$

where F_t [N] is the module of the force developed by the tire, F_χ [N] is the maximum force that the tire can support in certain conditions and F_γ [N] is the extra force that the tire could support in a determined instant.

Another important thing that can be extracted from (3.3b) is that the radius of the circle is directly related to the vertical load through the friction coefficient variable. A more detailed friction circle is shown in Figure 3.9.

3.4.2 Slip Ratio - Longitudinal Force

Slip ratio is defined, by SAE J670¹, as the difference between the angular velocity of a driven (or braked) wheel, ω_t [rad/s], and the angular velocity of the free-rolling wheel, $\omega_0 = v_{xt}R_t$. By using that definition, slip ratio σ can be expressed as

$$\sigma = \frac{\omega_\omega R_\omega - v_{xt}}{\omega_\omega R_\omega}, \quad (3.4)$$

where v_{xt} [m/s] is the longitudinal velocity of a determined tire and R_ω [m] is the radius of the tire itself. By using that definition, it can be concluded that slip ratio is positive ($\sigma > 0$ [%]) while accelerating and negative ($\sigma < 0$ [%]) while braking.

¹More information is available in https://www.sae.org/standards/content/j670_200801

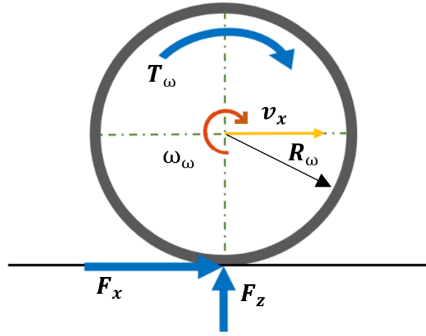


Figure 3.6: Wheel Dynamics

Figure 3.6, together with

$$J_\omega \dot{\omega}_\omega = T_\omega R_\omega - F_x, \quad (3.5)$$

where J_ω [kg/m²] is the wheel inertia and $\dot{\omega}_\omega$ [rad/s²] is the angular acceleration of the wheel, are useful to represent how the slip ratio depends on the torque delivered and the F_x from the track affecting the tire. Notice that the tire rolling resistance is neglected.

The effect of slip ratio together with the tires vertical load (Section 3.4.4) and by using the Pacejka's Magic Formula [Pacejka, 2008], allows to establish a proper parametrization of the longitudinal force of the tire as shown in Figure 3.7.

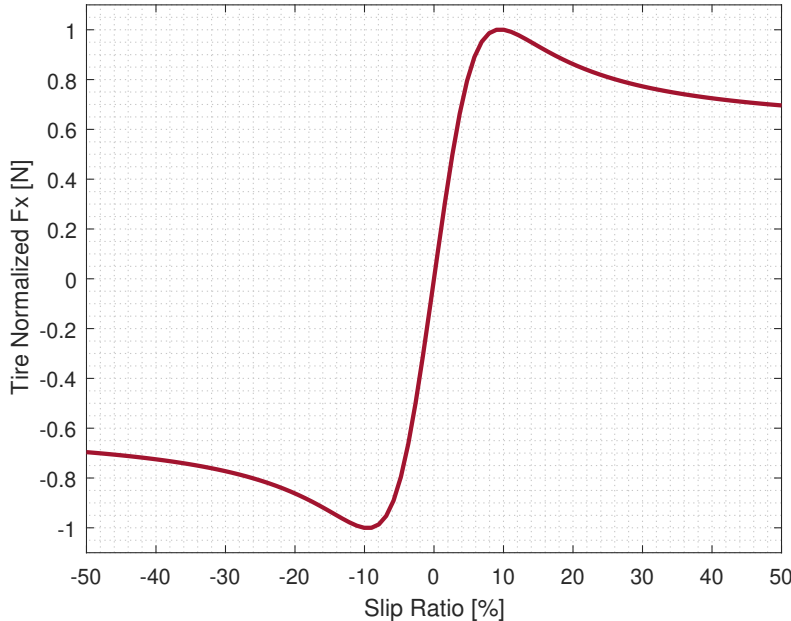


Figure 3.7: Longitudinal Force vs Slip Ratio

From Figure 3.7, it is notorious the change in the longitudinal force of the tire depending on its slip ratio for a determined vertical load. The optimal value (taking the positive value,

but symmetric for a braking situation) is found between 7% and 12 %, which means that the target torque for the motor of a wheel should take into account those constraints to take the maximum performance out of each tire.

3.4.3 Slip Angle - Lateral Force

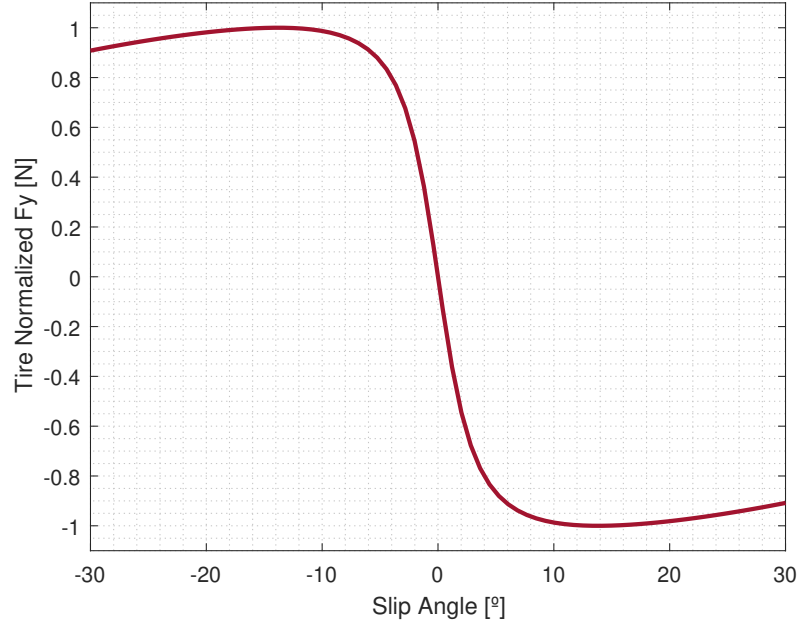


Figure 3.8: Lateral Force vs Slip Angle

Slip angle is defined as the angle between the forward direction of the tire and its actual velocity direction.

From Figure 3.8, it is also notorious the change in the lateral force of a tire depending on its slip angle for a determined vertical load. The optimal value is found (taking the positive values, but symmetric the negative ones) between 8% and 18 %. In this case, the driver is the one in charge of maintaining an optimal slip value in case a lot of lateral force is needed. It is important to notice that the target torque for the motor has also to take into account that value, because the maximum longitudinal force that the tire can handle is limited by the friction circle (Section 3.4.1).

Considering all the variables mentioned above, a complete friction circle is presented in Figure 3.9, which shows F_x and F_y limits depending on slip ratio and slip angle at a fixed F_z , temperature, pressure and friction coefficient.

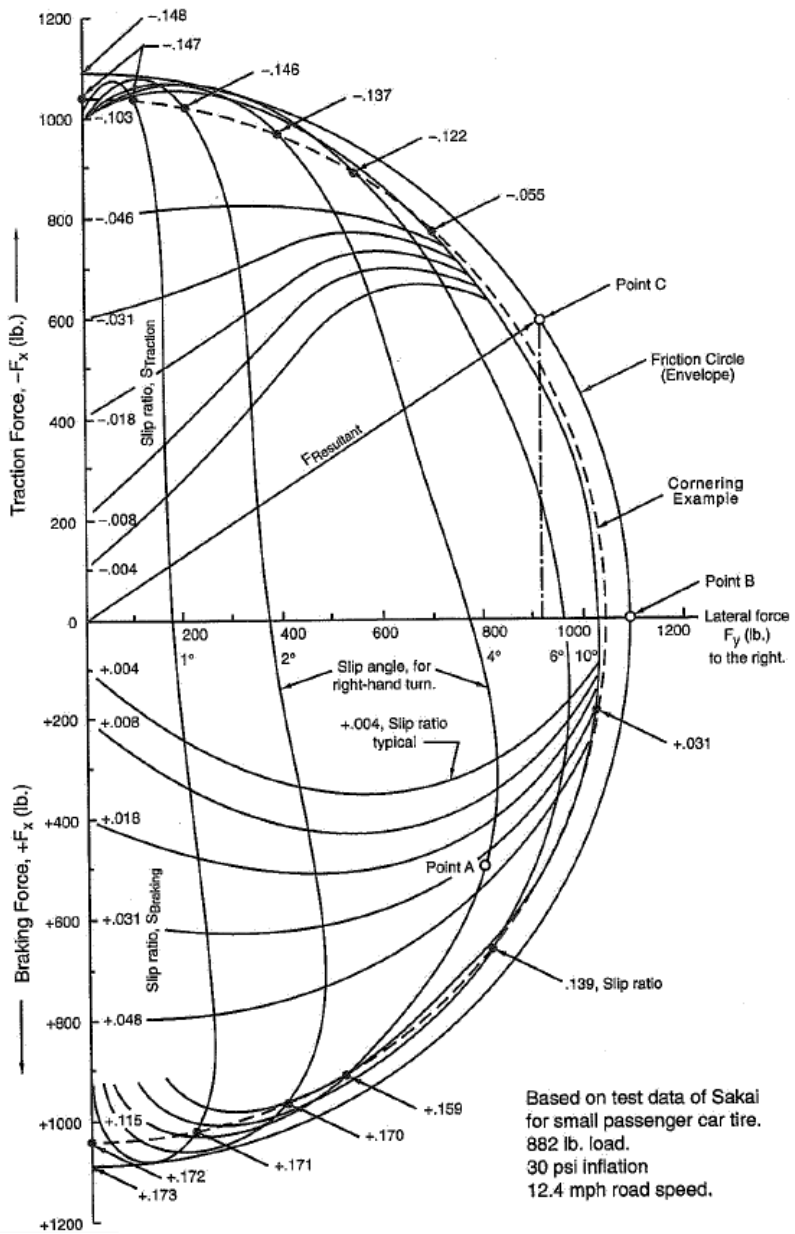


Figure 3.9: Complex Friction Circle Diagram [Mil, 1994]

3.4.4 Vertical Force

As shown in (3.3b), the maximum force that the tire can handle is directly related to its vertical force (or load). That fact implicitly explains why high vertical loads affecting the tire (without overloading it) are usually desired. Here, it is also possible to see why aerodynamics is so important in competition vehicles, as it allows to increase the normal load on a tire without the necessity of increasing the vehicle's weight.

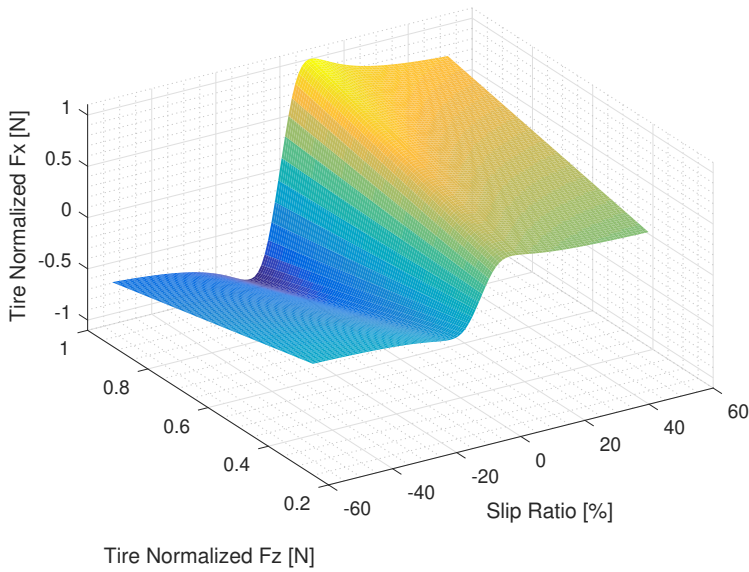


Figure 3.10: Normalized F_x vs Slip Ratio for multiple tire loads - 3D Graph

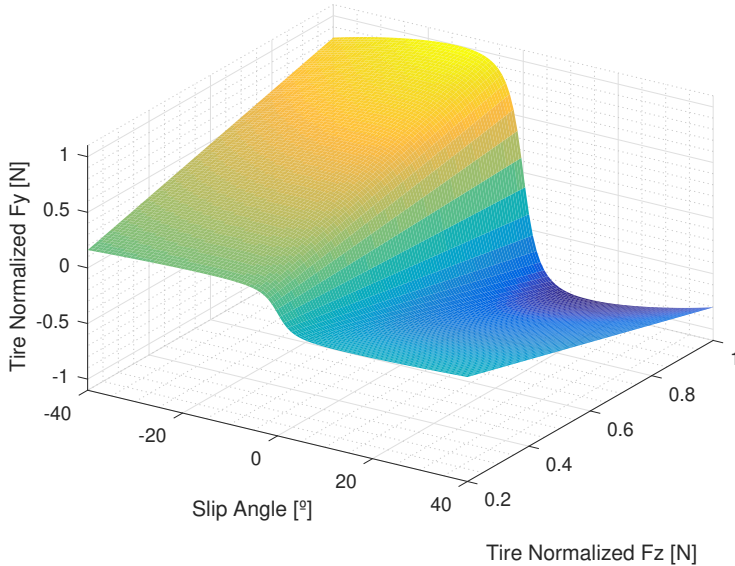


Figure 3.11: Normalized F_y vs Slip Angle for multiple tire loads - 3D Graph

To understand in a better way how the load affect the friction circle, Figures 3.10 and 3.11 are presented. In Figure 3.10 it is shown how, for a determined slip ratio, the value of the longitudinal force that a tire can develop increases together with the vertical load supported by the tire. An important consideration is that the longitudinal and lateral forces are directly related but not proportionally, as the friction coefficient value tends to reduce its slope together with the increase of load [Mil, 1994], otherwise the tire would be able to manage infinite

torque for an infinite value of vertical load. Similarly happens with the lateral force that a tire can handle for a fixed slip angle if the vertical load increases, however, another secondary consequence when the vertical load occurs related to the optimal slip angle, a concept called *tire sensitivity* explained in Section 3.4.5.

3.4.5 Ackermann Steering Geometry

As mentioned in Section 3.4.4, the driver is responsible of maintaining the slip angle at a right working range of values, but it cannot be done if the steering system is not correctly designed. It is important to know that the tire behaviour has a lot of influence over the design of this mechanical system. The importance of this component is, in part, due the tire sensitivity, which mainly explains one of the non-linear behaviour characteristics from each tire model itself.

The main consequence of the tire sensitivity is that the tire load modifies the optimal working slip angle value due to a compression in the rubber internal structure. To solve that problem, and try to maintain the tires working over optimal conditions, it exists the Ackermann steering geometry, which cause that the inner and outer steering angles are different², and which values are expressed as follows:

$$\alpha_{in} = \arctan \left(\frac{L}{\rho - \frac{t_f}{2}} \right), \quad (3.6a)$$

$$\alpha_{out} = \arctan \left(\frac{L}{\rho + \frac{t_f}{2}} \right), \quad (3.6b)$$

where α_{in} [rad] is the inner wheel steering angle and α_{out} [rad] is the outer wheel steering angle.

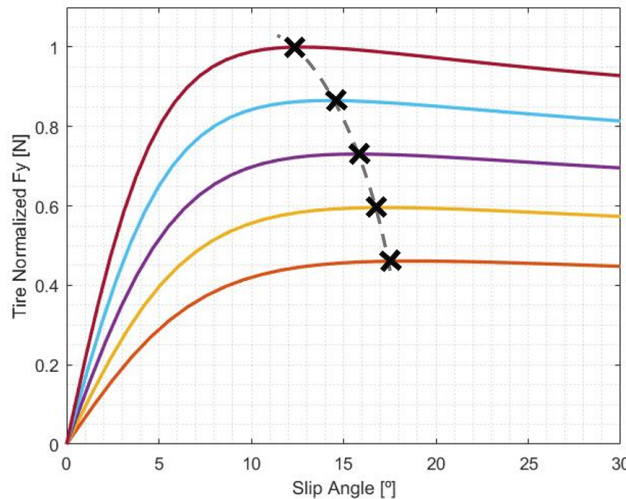


Figure 3.12: Pro-Ackermann Tire Characteristic

²Invented in Munich in 1817 by Georg Lankensperger, and patented by Rudolph Ackermann in 1818.

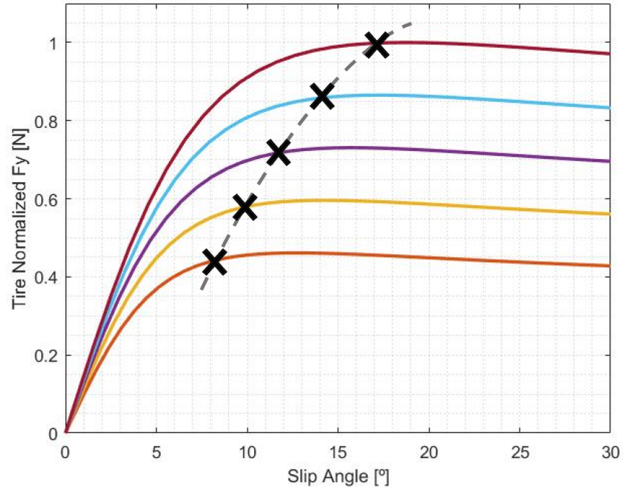


Figure 3.13: Anti-Ackermann Tire Characteristic

In Figures 3.12 and 3.13, the need of the Ackermann steering geometry is shown. Due to the lateral load transfer in a turning situation, the outer tire vertical force increase, while the inner ones decrease. The tire that is going to contribute the most in terms of lateral forces is going to be most loaded one, while with the other, the intent is going to be *maximizing the lateral force it can develop*. Because of the tire sensitivity, it is important to know the characteristic curve of a tire, and design an according steering system.

In Figure 3.14, it is shown how slip angles also determine the *Instant Center of Rotation* of the vehicle, comparing it with the ideal one without considering slip angles. That virtual point is important to being able to know the curve radius that the car may be able to handle at multiple velocities.

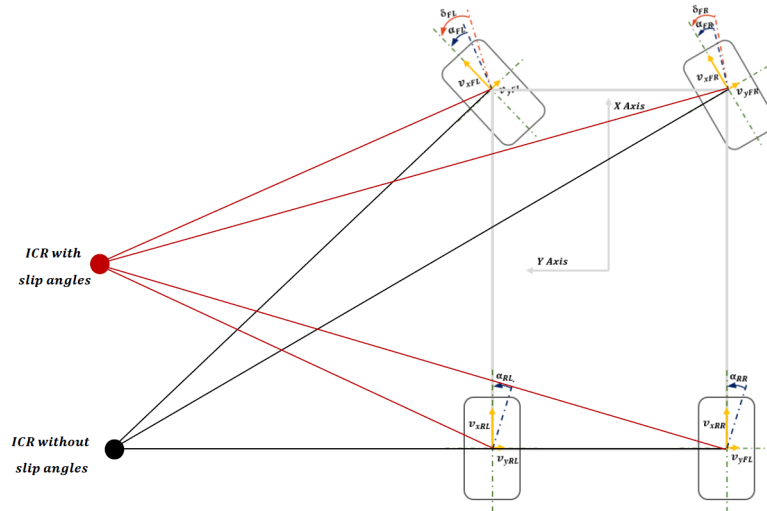


Figure 3.14: Idea vs real ICR

3.5 Three-Degrees-of-Freedom Bicycle Model

This is a commonly used model regarding to studies with automotive purposes, as it allows to study quite faithfully the yaw behaviour of a vehicle³. This dynamic simplification, useful as the integration can be quickly calculated, includes the longitudinal and lateral velocities, together with the yaw angular one, assuming symmetrical behaviour between left and right sides, while it neglects the effects of load transfer or aerodynamics. It also assumes small angles such as $\cos(\delta) \approx 1$ and $\sin(\delta) \approx \delta$ as this parameter $\in [-0.506, 0.506]$ rad.

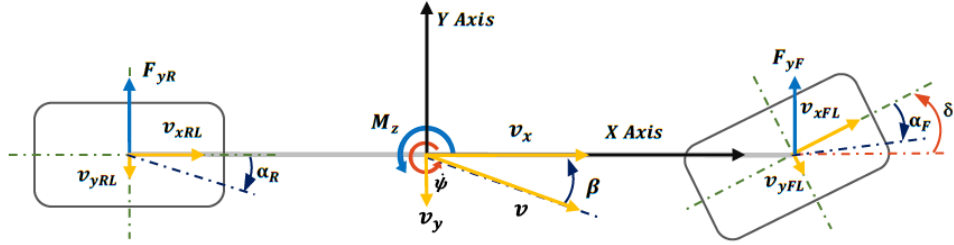


Figure 3.15: Bicycle Model Diagram

Using the schematic in Figure 3.15, it can be determined the dynamics of the system, expressed in the following equations:

$$a_y = \ddot{\psi} + \omega^2 \rho = v \dot{\beta} + v \dot{\psi}, \quad (3.7a)$$

$$m v (\dot{\beta} + \dot{\psi}) = F_{yF} + F_{yR}, \quad (3.7b)$$

$$J_v \ddot{\psi} - M_{z,TV} = l_f F_{yF} - l_r F_{yR}, \quad (3.7c)$$

where $\dot{\psi}$ [rad/s] is the yaw rate, $\ddot{\psi}$ [rad/s²] is the way acceleration and $M_{z,TV}$ [Nm] is the extra momentum around the Z axis due to the TV.

There is an important point to take into account when using this model, and that is the linearization of the tire behaviour, which, in fact, is something not desired to maintain constant in this project and is going to be modified in Section 4.3.

As it has been presented before, tire forces do not have a linear behaviour when relating them with slip angles. Linearizing them implicitly means that although the model is highly valid for *normal* driving maneuvers, or which is the same, when slip angle values are small, the error between the model and reality increases when talking to *aggressive* driving, the one in which this study is more addressed to. The calculus of each of the front slip angles is presented as follows:

$$\alpha_F = \beta + \frac{l_f \dot{\psi}}{v} - \delta, \quad (3.8a)$$

$$\alpha_R = \beta - \frac{l_r \dot{\psi}}{v}, \quad (3.8b)$$

³The $M_{z,TV}$ referenced in the axis center is the TV output.

where α_F [rad] is the slip angle of the front axis, α_R [rad] is the slip angle of the rear axis, β [rad] is the slip angle at the center of gravity (*CoG*) of the vehicle, l_f [m] is the distance between the *CoG* and the front axis, l_r [m] is the distance between the *CoG* and the rear axis, v [m/s] is the velocity of the vehicle at the *CoG* and δ [rad] is the mean of the steering angle values of the front tire.

A relevant parameter is included here, the *Cornering Stiffness*⁴, which is defined as the ability of the tire to resist deformation while a vehicle corners, which also means that it is the slope of the curve in Figure 3.11 (as $F_{yi} = -C_i \alpha_i$), which value could be considered as a constant only for slip angle values $\sigma \in [-8,8]$ degrees for the exposed tires.

By substituting (3.8a) and (3.8b) into (3.7b) and (3.7c,) and rearranging them, it can obtained the ones that determine the state space of our model presented as follows:

$$\dot{\beta} = \frac{-(C_f + C_r)}{mv} \beta - \left(1 + \frac{C_f l_f - C_r l_r}{mv^2}\right) \dot{\psi} + \frac{C_f}{mv} \delta, \quad (3.9a)$$

$$\ddot{\psi} = \frac{C_r l_r - C_f l_f}{J_v} \beta - \frac{C_r l_r^2 + C_f l_f^2}{J_v v} \dot{\psi} + \frac{C_f l_f}{J_v} \delta + \frac{M_{z,TV}}{J_v}, \quad (3.9b)$$

where C_f [N/rad] is the equivalent cornering stiffness for the front axis, C_r [N/rad] is the equivalent cornering stiffness for the rear axis and J_v [kg m^2] is the inertia of the vehicle around the Z axis, $\dot{\psi}$ [rad/s] is the yaw rate and $M_{z,TV}$ [Nm] is the moment due to the TV output.

State Space Equations

The inputs of the system are the steering angle at the wheel (δ), determined by the driver, and an extra torque around the Z axis of the vehicle ($M_{z,TV}$), which is the control output, so $u = \begin{pmatrix} \delta \\ M_{z,TV} \end{pmatrix}$. The states are the vehicle side slip angle (β) and its yaw rate ($\dot{\psi}$), so $x = \begin{pmatrix} \beta \\ \dot{\psi} \end{pmatrix}$. With this brief introduction and (3.9a) and (3.9b), the following state-space model is presented:

$$\dot{x} = \begin{pmatrix} \frac{C_r l_r - C_f l_f}{J_v} & -\left(1 + \frac{C_f l_f - C_r l_r}{mv^2}\right) \\ \frac{-(C_f + C_r)}{mv} & \frac{C_r l_r^2 + C_f l_f^2}{J_v v} \end{pmatrix} x + \begin{pmatrix} \frac{C_f}{J_v} & 0 \\ \frac{C_f l_f}{J_v} & \frac{1}{J_v} \end{pmatrix} u, \quad (3.10a)$$

$$\dot{y} = \begin{pmatrix} 1 & 0 \\ 0 & 1 \end{pmatrix} x + \begin{pmatrix} 0 & 0 \\ 0 & 0 \end{pmatrix} u. \quad (3.10b)$$

⁴Notice that in this model, both parameters refer to the stiffness of both left and right tires in the same axle.

At this point, it is important to be aware of the intrinsic considerations of this model which are presented here:

- There is an implicit partial loss of information due to the linearization of the tire forces.
- The δ value is the mean value of the relation between the steering angle and the wheel turning angles.
- The mass m includes the mass of the vehicle together with the one corresponding to the driver, which might not always be the same.

Because only one model, with a determined velocity and constant cornering stiffness value, is not sufficient to include all the information needed to satisfy the requirements for the control design, a different approach is going to be done regarding to the simple bicycle model, proposing a Linear Parameter-Varying (LPV) bicycle model Section 4.3.

The proposed approach is going to be based in a function for the cornering stiffness of the tire together with multiple velocity values. This is going to be included in the simple bicycle model, which performance is going to be dependent on the scheduling variables of that proposed LPV model (Section 4.3).

3.6 Vehicle Behaviour/Sensitivity

The understeer and oversteer terms are used to determine the vehicle sensitivity when cornering. To firstly present it in a simple way, this term is used to refer to the car reaction when there is the intent of cornering from the driver.

Understeering (Figure 3.16) produces when the car turns less than commanded by the driver and oversteering (Figure 3.16) when it turns more. Just as a detail, it is not completely correct to talk about understeering or oversteering vehicles. There are understeering and oversteering situations, and a car may have tendency to respond one way or another. The technical explanation for this behaviour is going to be based in the approach extracted from [Han, 2015].

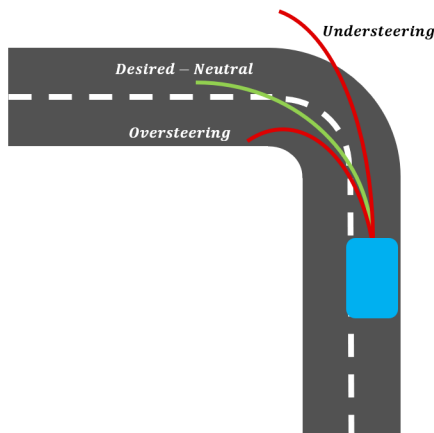


Figure 3.16: Understeering and Oversteering Scheme

Neutral, Understeering and Oversteering

Firstly, it is important to present that the turning radius ρ is calculated as follows [Han, 2015]:

$$\rho = \left(1 - \frac{m(C_f l_f - C_r l_r) v^2}{l^2 (C_f C_r)} \right) \frac{l}{\delta}. \quad (3.11)$$

Equation (3.11) is plotted in Figure 3.17 to show how the turning radius varies depending on velocity for a fixed steering angle δ value in steady-state cornering.

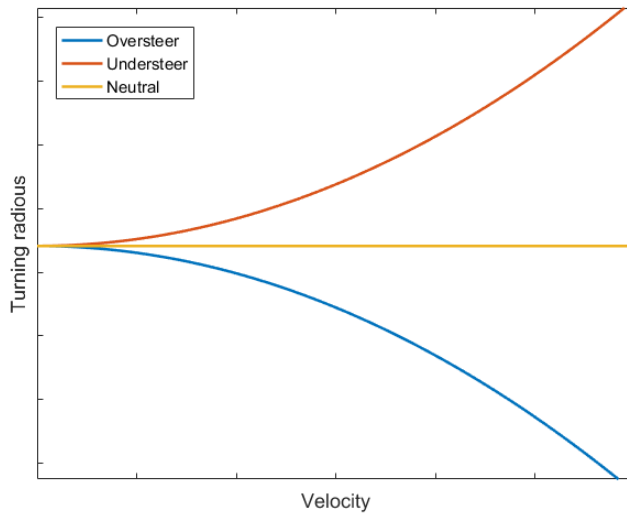


Figure 3.17: Understeering, Oversteering and Neutral Plot Example

The explanation of that behaviour lies on the $C_f l_f - C_r l_r$ term. The first observation to be done is that for a constant steer angle, if $C_f l_f - C_r l_r = 0$, the radius of the vehicle is not related to velocity and is constant with a value of $\rho = \frac{l}{\delta}$ at any velocity. That is a neutral behaviour.

- When $C_f l_f - C_r l_r < 0$, the car is understeering. In the graph it is shown how the turning radius increases together with velocity, which means that it *turns less* for an equal steering angle value. In this case, the steering angle value should increase in order to maintain the same turning radius.
- When $C_f l_f - C_r l_r > 0$, the car is oversteering. In the graph it is shown how the turning radius decreases together with velocity, which means that it *turns more* for an equal steering angle value. In this case, the steering angle value should decrease in order to maintain the same turning radius.

There are other methods to examine this behavior. An interesting one is doing it by the analysis of slip angles. While in a neutral situation front and rear axles slip angles are nearly the same, when understeering, the value of the front slip angle is higher than the rear one and the other way round when oversteering. This approach is explained in more detail in [Han, 2015].

3.7 Vehicle Data Analysis

According to Jörge Segers, “*An activity that is not measured, cannot be controlled nor managed*” [Segers, 2008]. In motorsport, the most important thing to take into account is the stopwatch, as it gives a global vision of the performance of the driver together with the car.

The feeling of a driver and his/her observations are always important aspects to take into account, however, some of them are always subjective. Nowadays, motor-sport engineers have lots of information to analyze, which is incredibly useful to objectively determine quality of the performance of a vehicle (as mentioned, always keeping in mind the comments of the driver). A part from being useful for performance analysis, it can also be useful to analyze issues or whatever desired regarding to the vehicle. With a great amount of information, the person in charge of the analysis is responsible of knowing nearly every single detail of the studied car, just to know what to look for.

3.7.1 Data Acquisition

All the information in the CAT12e is transmitted via Controller Area Network (CAN), a quite common communication protocol used in the automotive industry. The prototype is equipped with a self-developed data logger, which main objective is to keep all the desired data measured by the vehicle sensors to be analyzed offline. In addition to the capacity of storing the desired data, the vehicle also disposes of a telemetry module used to receive real-time information which allows to determine whether essential components are working the right way.

All the sensors implemented on the car (Section 3.7.2) have both analytics and controllable purposes. There is a great variety of sensors available, and a suitable research must be done in order to select the ones that best suit the necessities, which means that a balance between quality and cost is an important task to be done.

3.7.2 Sensors and actuators

Inertial Navigation System - INS

The INS used was the Ellipse 2-N model from SBG Systems (Figure 3.18). This sensor is placed as near as possible from the CoG of the vehicle. It gives some of the most important information needed for the control algorithm of the car such as the $\dot{\psi}$, v_x , v_y , a_x and a_y . It is also used to determine the position of the car inside a track, which allows to know whether it is passing through a curve or a straight inside it.



Figure 3.18: Ellipse 2-N

Inertial Measurement Unit - IMU



Figure 3.19: MTLT305D

The IMU used was the MTLT305D model from ACEINNA (Figure 3.19). It is mostly used to accurate the process of data analysis when studying the front and rear axles behaviour together with vertical forces and lateral load transfer calculation purposes.

Lineal Position Sensor



Figure 3.20: Lineal Position Sensor

Position sensors (Figure 3.20) is used for three main objectives. It allows to measure the vertical load on each tire by measuring the elongation of the suspension springs, it is also used to measure the steering rack position to know the steering wheel angle and the pedal position which determines the torque command.

Resolver

The resolver used was the RE-15 model from LTN ServotechniK (Figure 3.21). It is quite a sensible sensor able to measure the electrical machines rotational speed, crucial for the control process and also for calculation regarding to slip ratio or control algorithms such as the traction control.



Figure 3.21: Resolver RE-15

Electrical Machines



Figure 3.22: Fischer Electrical machines

CAT13e is equipped with four Fischer electrical machines (Figure 3.22) specifically designed for Formula Student prototypes. Its peak power is 35 kW with a maximum available torque of 29 Nm and maximum speed of 18000 rpm.

Inverter



Figure 3.23: MOBILE DCU 60/60

CAT13e is equipped with two MOBILE DCU 60/60 double inverters (Figure 3.24) for the control of the electrical machines, one for each front and rear car axis. Its internal fast controllers ensure that the target torque is always reached.

Energy Meter

CAT13e is equipped with an Isabellenhütte IVT-MDOULAR energy meter sensor, which allows to take useful data about battery voltage, intensity, power or even energy consumption.

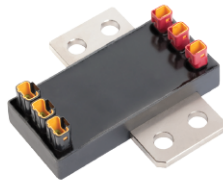


Figure 3.24: Isabellenhütte IVT-MODULAR

3.8 Data Analysis Software

Data analysis has become highly useful and a remarkably important task that helps a lot in determining a vehicle behaviour. It sometimes requires time and precision, and it is highly evolving thanks to the dedicated sensors that enable the measurement of each variable to analyze.

In ETSEIB MotorSport, the software DataAnalysisPro (GEMS Performance Electronics⁵) is used for this specific task. It allows to import and treat the logged data from the vehicle and organize that data depending on their purposes. The most beneficial feature is, as mentioned, the possibility to treat data and also to plot them in multiple graphs for different characteristics to be analyzed.

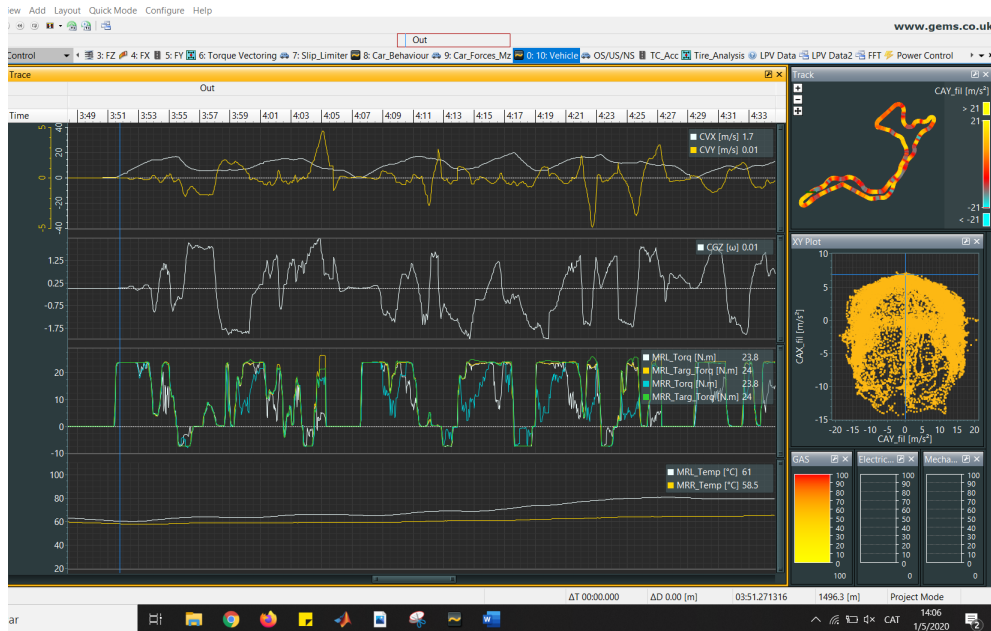


Figure 3.25: DataAnalysisPro Example

In Figure 3.25, an example of the analyzed data is shown, in which velocities, accelerations or motor torques graphs can be analyzed.

⁵<https://gems.co.uk>

The data analysis software is useful to analyze a lot of important information. However, when data must be treated, for example, to obtain graphs or parametric curves such as the tyre ones presented in Chapter 3, MATLAB is a crucial software to achieve the desired results.

3.9 Summary

In this chapter, a brief introduction of some technical aspects over vehicle dynamics are presented. Some information is about general dynamics and some is about essential topics considered important to be presented here in order to enhance a better understanding of them and the reason of why and how they are used in the following sections of this project.

The majority of the figures regarding data are obtained from a post-treatment of information obtained during tests or competitions with the CAT12e vehicle. For that reason, all the sensors needed for the obtainment of such data and the software used to analyze it have been presented.

Chapter 4

Yaw Rate Control-Oriented Dynamic Model

4.1 Problem Statement

CAT13e, the formula student electric vehicle of the team ETSEIB MotorSport, is driven by four independent electrical machines, one mounted in each of the four wheel assemblies. They are controlled by the output signals from the two motor controllers mounted on the vehicle, one in charge of each of the two axles. A simple, and also highly inefficient way to send the torque set points for each machine would be sending the 25% of the commanded torque by the driver to each of them, but vehicle and tire limitations would not be taken into account, so it would lead to excessive tire wear, inefficient energy management, poor vehicle performance and difficulties while driving.

The aim of the TV algorithm, including the yaw rate controller (Chapter 5) and the TD problem (Section 6.3), is to take the vehicle limitations, together with the tire ones, into account, and by doing so, maximize the vehicle performance while minimizing the wear of the tire and the energy waste. All those improvements are considered together with the ability to adapt the vehicle to the technique of driving of the driver. There are three crucial parts which shape the whole TV algorithm outlined below.

- Yaw Rate Control-Oriented model:

The design of a model to further design the following controller is needed. A quite used model to study the yaw behaviour of the car is the *Three-Degrees-of-Freedom Bicycle Model* presented in Section 3.5, but it intrinsically includes some limitations which are going to be partially suppressed with the design of a more complete Quasi-Linear Parameter Varying Bicycle model, presented in Section 4.3.

- Proportional-Integral Yaw Rate Controller:

A controller is needed to fit the behaviour of the car together with the driver intentions in cornering conditions. To achieve this goal, a proportional-integral-type yaw rate controller is designed (Chapter 5), whose output is going to determine the most adequate $M_{z,TV}$ for the vehicle actuators to generate.

- Torque Distribution Problem:

Once the driver inputs have been transformed to control signals (M_z^{ref} and F_x^{ref}), the last step is to enable the car to correctly interpret those signals and send the correct targets to each one of the actuators, always taking into account the vehicle limitations. To achieve that goal, a TD problem (Section 6.3) is designed.

This three main components of the whole TV are presented in the following chapters together with the obtained results and conclusions that can be extracted from them.

4.2 Linear Parameter Varying Model

The Linear Parameter-Varying (LPV) concept was firstly introduced by Jeff S.Shamma in 1988 [Shamma, 1988]. It is defined as a finite-dimensional linear time-varying plant whose state-space matrices are functions of a vector of varying and measurable parameters, which are called scheduling variables.

The intrinsic objective of this modelling approach is to include the physics of a non-linear system in a set of linear sub-systems obtained by linearizing the model around multiple operating conditions. An LPV model is defined as

$$\begin{aligned} x^+ &= A(\phi) x + B(\phi) u, \\ y &= C(\phi) x + D(\phi) u, \end{aligned}$$

where x^+ is the evolution of the states, y is the variation of the measured outputs, $x \in \mathbb{R}^{n_x}$ is the input vector, $y \in \mathbb{R}^{n_y}$ is the output vector, $u \in \mathbb{R}^{n_u}$ is the control signals vector, $\phi \in \mathbb{R}^\phi$ are the scheduling variables and $A(\phi) \in \mathbb{R}^{n_x \times n_x}$, $B(\phi) \in \mathbb{R}^{n_x \times n_u}$, $C(\phi) \in \mathbb{R}^{n_y \times n_x}$ and $D(\phi) \in \mathbb{R}^{n_y \times n_u}$ are the state-space time-varying matrices of suitable dimensions.

At this point, it is important to take into account the simple bicycle model presented in Section 3.5 and the linearizations it entails. As the vehicle in which this study is focused on is of competition-type nature, in which the endogenous non-linearities of the system tend to be more relevant compared, for example, with a road car, there is a higher necessity to consider them somehow to favor a better control design.

As a result of using the LPV approach, a non-linear system can be controlled by a collection of linear controllers adapted to each working point (operating condition).

4.2.1 LPV Model Types

An important aspect to take into account is the nature of the scheduling variables that are going to determine the working condition. Depending on that, there are two types of LPV models presented below [Marti Rubio, 2016, Rotondo et al., 2013]:

- Pure LPV Model:

It is defined as a system in which the scheduling variables depend on exogenous signals.



- Quasi LPV Model:

It is defined as a system in which the scheduling variables can depend on both exogenous and endogenous signals, such as states, inputs or outputs.

There are other approaches when designing a state-space model, which are linear time-invariant models (LTI) and linear time-variant models (LTV), whose differences over the LTV models are briefly discussed in Sections 4.2.2 and 4.2.3.

4.2.2 LTI vs LPV

A Linear Time Invariant (LTI) model is defined as

$$\begin{aligned} x^+ &= Ax + Bu, \\ y &= Cx + Du, \end{aligned}$$

where A , B , C and D are the time-invariant matrices of suitable dimensions.

LTI systems are a kind of systems in which the output value is a linear combination of its inputs. Moreover, what defines this kind of systems is the fact that the output value does not depend on *when* an input is applied. This characteristic, in fact, is which differences it from an LTV system (and, as a consequence, from an LPV one).

4.2.3 LTV vs LPV

A Linear Time-Varying (LTV) model is defined as

$$\begin{aligned} x^+ &= A(\phi)x + B(\phi)u, \\ y &= C(\phi)x + D(\phi)u. \end{aligned}$$

As mentioned above, the difference between LTI and LPV systems is clear, however, the difference between LTV and LPV is less apparent. In fact, an LPV system is a kind of system included in LTV systems group. The distinction between those is in the perspective taken on analytics and synthesis. In an LTV, the time-varying parameters depend on time itself, while in LPV, the time-varying variables depend on parameters that can be measured or estimated and can vary over time.

4.3 Quasi-LPV Bicycle Model

The objective of the model proposed below is to fill some of the *blank spaces* that unavoidably determine the limitations of a simple bicycle model presented in Section 3.5.

This approach models the non-linear behaviour of a vehicle by linearizing that behaviour around multiple working conditions defined by the scheduling variables v and β . It is important to know that the non-linear characteristics are embedded in those variables. By doing so, both the velocity and the car sensitivity are considered, a fact that is going to allow to obtain a more concordant model referring to the real vehicle. The general description of the model is presented as follows:

$$\beta^+ = \frac{-(C_f(\beta) + C_r(\beta))}{m v} \beta - \left(1 + \frac{C_f(\beta) l_f - C_r(\beta) l_r}{m v^2}\right) \dot{\psi} + \frac{C_f(\beta)}{m v} \delta, \quad (4.1a)$$

$$\dot{\psi}^+ = \frac{C_r(\beta) l_r - C_f(\beta) l_f}{J_v} \beta - \frac{C_r(\beta) l_r^2 + C_f(\beta) l_f^2}{J_v v} \dot{\psi} + \frac{C_f(\beta) l_f}{J_v} \delta + \frac{1}{J_v} M_{z,TV}, \quad (4.1b)$$

where the stiffness coefficients of the front axle (C_f) [N/rad] and the rear axle (C_r) [N/rad] are determined by the following expression:

$$C_\gamma(\beta) = \frac{\mu_t \alpha_t}{\gamma_t \beta_t^2 + \delta_t}, \quad (4.2)$$

where C_γ refers to the cornering stiffness of the front ($\gamma = f$) or rear axle ($\gamma = r$), β_t [rad] is the slip angle of the tire and μ_t , α_t , γ_t and δ_t are tuning parameters which depend on the tire model and must be selected based on analyzed data focusing on the sensitivity of the vehicle.

The non-linear relation between the cornering stiffness and the slip angle explains why it has been considered important to introduce a weighing relation between front and rear cornering stiffness.

In a previous data analysis, it has been observed that a bicycle model cannot take into account the tendency to understeer or oversteer that a vehicle may present. To solve that problem, an extrapolation of the tire behaviour is proposed. By including the dependency of the beta in the cornering stiffness values, the vehicle sensitivity can be taken into account. Another important consideration is that the front and rear stiffnesses are weighted.

To make a brief introduction of the model results, a comparison between real data, a bicycle model including the velocity effects and another including the velocity and the slip angle ones is presented in Figure 4.3. The analysis was done over real Skidpad data, and it is observable that, by introducing the β dependency, the modelling results improve considerably.

An interesting observation that can be extracted from the comparison in Figure 4.1 is that the proposed Quasi-LPV model (4.1) fits the real data around 20% better than it would if the vehicle sensitivity was neglected, as the simple bicycle model tends to present a considerably higher oversteering behaviour for the same model due to its constant cornering stiffness value.

LPV Bicycle Model Validation

Once the model is designed, the following step consists in its validation. To do so, the process starts by experimentally analyzing the error, calculated as

$$\epsilon_{rel} = 100 \sqrt{\frac{\sum_{i=1}^{n_R} (R - M)^2}{\sum_{j=1}^{n_R} R^2}}, \quad (4.3)$$



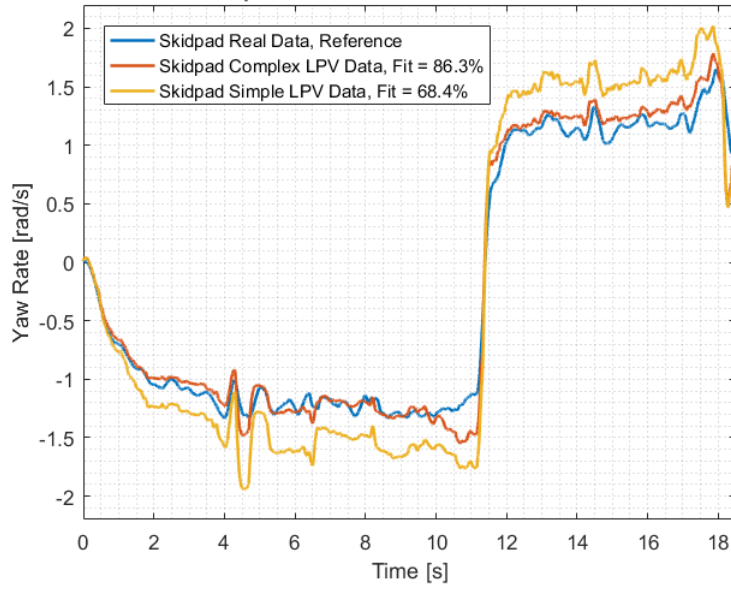


Figure 4.1: Comparison between simple bicycle model and Quasi LPV bicycle model

where $R \in \mathbb{R}^{n_R}$ is the vector of real data and $M \in \mathbb{R}^{n_M}$ is the vector of the Quasi-LPV model (4.1) data. In Figure 4.2, the computed error depending on the step size of the scheduling variable is shown. By the result of these plots, the most suitable step sizes have been selected, which are also determining the working conditions around which linearizing the whole model (4.1).

During that error study, it has been also observed that *extreme* step sizes did not work properly together. For example, at first view, a velocity step size of 8.3 m/s would be reasonably suitable (see Figure 4.2), but together with a angle step size of 0.018 rad or even 0.05 rad destabilize the system. From the obtained results and their interpretation, a velocity step size of $\Delta v=6.94$ m/s and $\Delta \beta=0.087$ rad have been selected for the rest of the study.

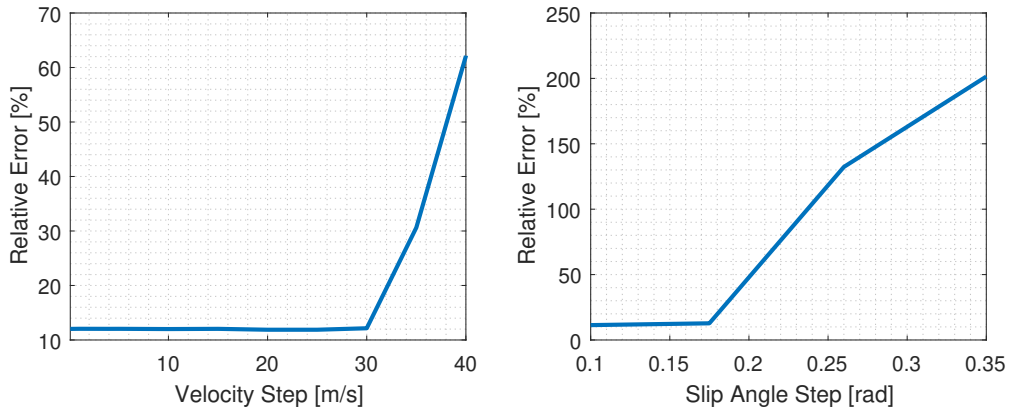


Figure 4.2: Relative error vs Scheduling Variables Step

To conclude with the validation, the output yaw rate data from the Quasi-LPV model in (4.1) has been compared with real data logged during the Endurance event held in the *Circuit the Barcelona, Catalunya* (Figure 4.4 represents some useful data where velocity and track profile are shown), during the 10th edition of Formula Student Spain. The data comparison is presented in Figure 4.3.

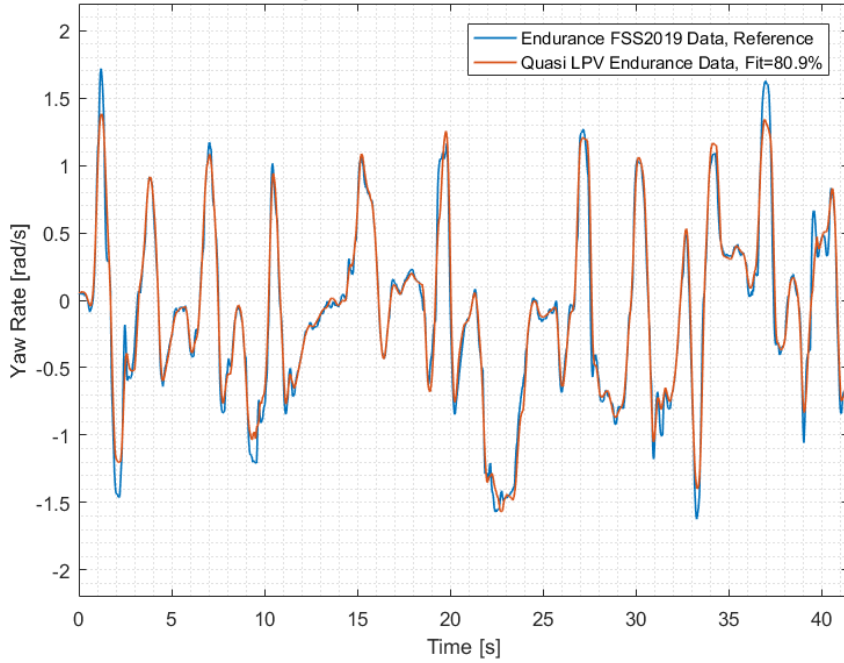


Figure 4.3: Comparison between real data and Quasi-LPV model

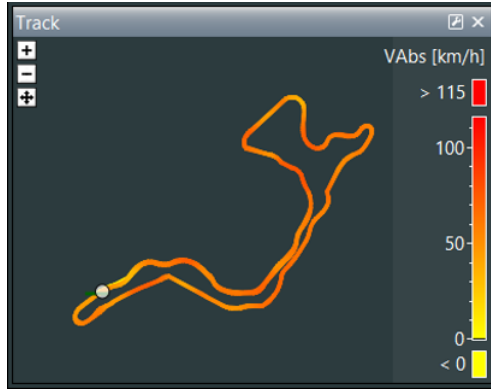


Figure 4.4: GPS Velocity during FSS Endurance

With the obtained results of the comparison above, it can be concluded that the model output corresponds quite faithfully with the measured data from the vehicle, so (4.1) is a suitable model to design a yaw rate controller.

Another important comparison between the model in (4.1) and the IPG-CarMaker simulator software is presented in order to corroborate that the data obtained from both models fit correctly (Figure 4.5) and to ensure that the automotive software is useful and correctly programmed for further simulations.

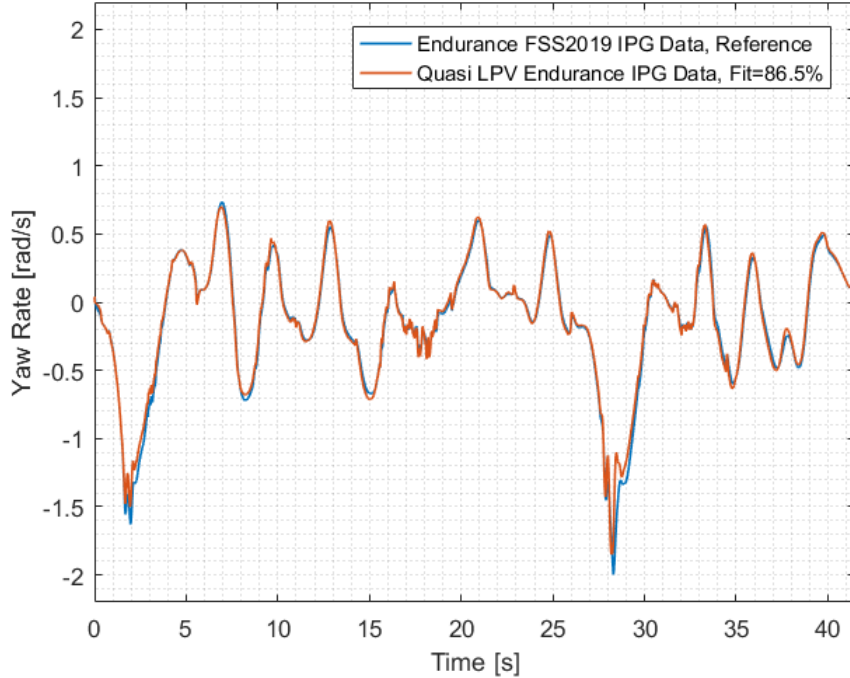


Figure 4.5: Comparison between IPG and Quasi-LPV model

With the obtained results, together with a previous works on validation between real data and the one extracted from the IPG-CarMaker around the FSS Endurance track (Figure 4.4), it can be concluded that this software is going to be useful for the final algorithm simulations exposed in Chapter 7.

4.4 Summary

In this chapter, the Quasi-LPV bicycle model (4.1) which is going to be used for further controller design objectives has been presented as a result of including the vehicle sensitivity into a simple bicycle model after analysing certain amount of data obtained during tests on track at multiple circuits. The validation process has also been presented together with the final comparison with real data to discuss the improvement that comes from the inclusion of the vehicle sensitivity in terms of data-fitting.

The last topic discussed in this chapter is a comparison between (4.1) and the simulation software IPG-CarMaker. This comparison is an important step that allows to ensure that the automotive software was correctly programmed for the TV simulations, crucial to obtain the final results of the project (Chapter 7).

Chapter 5

Yaw Rate Control Design

5.1 General Control Scheme

In this chapter the general control scheme (Figure 5.1), which main components were briefly described in Section 4.1, is presented, focusing on the first of those elements, the yaw rate controller. Firstly, it is important to describe each main part involved in the process of converting the driver inputs into adequate control signals. Starting from the driver inputs, they are used for two important objectives. The first one is the generation of the yaw rate reference (Section 5.2) and the other one is the effect those inputs are going to have in the TD problem over each motor. For every different situation, the TV (including both the yaw rate controller and the TD problem) is going to output four desired torques which are the set point torques for the inverter modules. Finally, the Kalman filter¹ [Blázquez Romañá, 2020] is an important input in the TV algorithm, as it gives information about the tires forces.

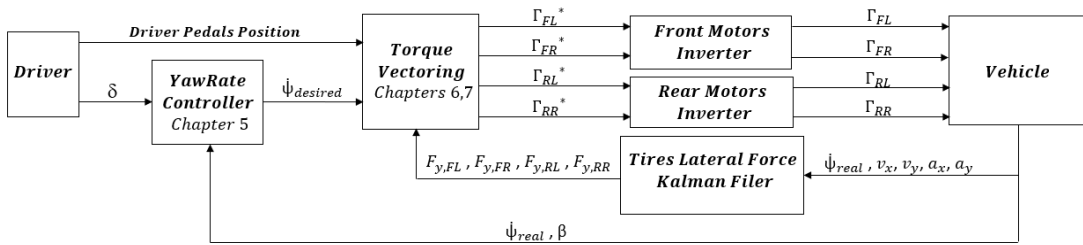


Figure 5.1: Control Scheme

5.2 Yaw Rate Reference Signal

Firstly, it is crucial to determine the objective of the controller. In this case, the performance of this control module is going to be determined in terms of its capacity to follow the yaw rate reference (Section 5.3) which the driver requests at every time and situation as fast as possible.

¹Estimators is a subject which remains out of the scope of this project.

Because of the desired approach that has been selected to determine the yaw rate reference, the bicycle model of Section 3.5 is going to be taken into account. There is a reason to use that model in this case, and it is because it has been preferred to select a constant relationship between the yaw rate reference and the steering angle value, which is the one that the driver can control. By doing so, it can be more natural for him/her to drive the vehicle. As a result, the relation between β and the cornering stiffness is neglected and a constant proportion for that variable is selected.

The transfer function $H(s) = \frac{\dot{\psi}(s)}{\delta(s)}$ is going to be presented in steady-state condition and rearranged. To obtain this transfer function, the bicycle state-space model (Section 3.5) has been used, and the following algebra has been applied over it:

$$\begin{aligned} X(s) &= (sI - A)^{-1} BU(s), \\ Y(s) &= C(sI - A)^{-1} BU(s). \end{aligned}$$

Applying that algebra allows to get the equation from state-space matrices as follows:

$$\frac{Y(s)}{U(s)} = C(sI - A)^{-1} B.$$

And the final rearranged definition for the $\dot{\psi}$ can be obtained as a function of δ as follows:

$$\dot{\psi} = \frac{1}{1 - \frac{m}{l^2} \frac{(C_f l_f - C_r l_r) v^2}{C_f C_r}} \frac{v \delta}{l}. \quad (5.1)$$

As seen in Section 3.6, the term $C_f l_f - C_r l_r$ defines the behaviour of the vehicle. Taking advantage of that relation, an *Understeering coefficient*, K_u , presented in [Han, 2015] is going to be introduced as follows:

$$K_u = -\frac{m}{l^2} \frac{(C_f l_f - C_r l_r)}{C_f C_r}. \quad (5.2)$$

This is simply a part of the denominator in (5.1), but it is going to be quite useful for control purposes. Making its substitution into (5.1), it finally results

$$\dot{\psi}_{ref} = \frac{1}{1 + K_u v^2} \frac{v \delta}{l}. \quad (5.3)$$

The usefulness of (5.2) relies on the fact that it allows to generate an understeer, oversteer or even neutral yaw rate reference, which is going to lead to the correspondent behaviour that the TV is going to try to achieve. The modification of the K_u value is going to make the vehicle quite adaptable to the driver ability. For $K_u > 0$, the $C_f l_f - C_r l_r$ is negative, so the generated reference is going to be an understeering one. On the other side, for $K_u < 0$, the $C_f l_f - C_r l_r$ is positive, so the generated reference is going to be an oversteering one.

Also referring to K_u , it is important, while designing a car, to have an *objective* K_u and make the correspondent design to get around it as much as possible. The reason for that is because, as the natural car behaviour approaches more that value, *less effort* is going to be needed

from the TV, which, at the end, results in less energy waste as the vehicle itself is more likely to perform as desired.

The yaw rate that a vehicle can handle is limited, so its maximum value has to be taken into account [Anton Stoop, 2014]. Taking (3.7a) and neglecting the $\dot{\beta}$ term due to its not much significant value compared to $\dot{\psi}$ and the difficulty to measure it, the equation of interest is

$$m a_y = m v \dot{\psi} \leq m \mu g. \quad (5.4)$$

So the resulting maximum affordable yaw rate that can be requested as a set-point for the controller is

$$\dot{\psi}_{max} = \frac{\mu g}{v}. \quad (5.5)$$

Finally, the set-point yaw rate for the controller is going to be

$$\begin{cases} \dot{\psi}_{ref} & |\dot{\psi}_{ref}| < |\dot{\psi}_{max}|, \\ \dot{\psi}_{max} & |\dot{\psi}_{ref}| \geq |\dot{\psi}_{max}|. \end{cases}$$

Is important to know that the value of the friction coefficient μ is time-variant and quite complicated to determine. However, it exists between a known range of values, so it can be tuned depending either on the track or situation.

5.3 Yaw Rate Controller Design

A Proportional-Integral-Derivative (PID) gain-scheduling-based [Karl Johan Åström, 2008] controller type has been selected because of its relative simplicity and the tuning flexibility it offers. It gives the possibility to slightly tune the parameters over a determined range to modify the behaviour depending on the driving characteristics of each driver, as CAT13e is not driven for only one person.

The controller is designed in discrete-time due the subsequent implementation on the main ECU of the vehicle, an ETAS ES910 Module², and it has the following general notation:

$$C_z(v, \beta) = K_p(v, \beta) + K_i(v, \beta) \frac{T_s}{2} \frac{z}{z - 1}. \quad (5.6)$$

The selection of a PI controller is due to the fact that a small rise time is desired (and obtained due the K_p) and the desire of eliminating the steady-state error in case is be necessary (and obtained due the K_i). A possible approach is also to consider only a proportional controller, as steady-state regime is rarely achieved with the car because it is constantly changing its yaw rate. The derivative component is not used due to the fact that the input signal $\dot{\psi}$ has high frequency noise and could be counterproductive.

The controller constants have been selected for each operating condition, all of them with the same control objectives, which are the following:

- Stability in all the working conditions.

²https://www.etas.com/en/products/es910_rapid_prototyping_module.php

- Least possible overshoot with a maximum value of 15 %.
- Least rise time. As the steady-state condition is not common while driving, it has been selected for the car to follow the reference as fast as possible.
- The least possible gain loss for the considered frequency range.

To obtain the above mentioned objectives, the *Control System Designer App* inside the *MATLAB Control System Toolbox*³ has been used. With the use of this application, a controller has been designed over each one of the linearized sub-models obtained from linearising (4.1) around the selected working conditions, and the parameters for each controller have been selected by analysing the correspondent step response, root locus graph and Bode plot. In Tables 5.1 and 5.2, each one of the constants for the controllers are presented together with their correspondent working point determined by the velocity and slip angle.

Table 5.1: K_p Values for multiple operating conditions

—	Slip Angle				
Velocity	-0.1745	-0.08730	0	0.0873	0.1745
0.2276	7525.5	23590	35162	23590	7525.5
7.2220	562.93	1415.7	1987.3	1415.7	562.93
14.166	543.14	1094.9	1376.8	1094.9	543.14
21.111	496.35	641.8	1079.7	641.8	496.35
28.055	348.7	540.64	885	540.64	348.7

Table 5.2: K_i Values for multiple operating conditions

—	Slip Angle				
Velocity	-0.1745	-0.08730	0	0.0873	0.1745
0.2276	739114	781540.8	1165007	781540.8	739114
7.2220	36887.4	36705.7	46413.14	36705.7	36887.4
14.166	24785.29	23873	25683.64	23873	24785.29
21.111	19723.5	19574.41	18683.2	19574.1	19723.5
28.055	17202.4	17553.16	14936.5	17553.16	17202.4

Figures 5.2 and 5.3 are presented below with the objective of showing the controller values dependency over the scheduling variables in a more graphical way.

There are two possible approaches for the implementation of the parameters inside the controller:

- A 2-Dimensional Look-Up Table:

It might be a suitable approach, but it must be previously ensured that the output behaviour of the parameter is continuous, does correspond with the correct values for

³<https://es.mathworks.com/products/control.html>

its input and no error is generated due to the linearization between the multiple brake-points of the array that conforms the look-up table.

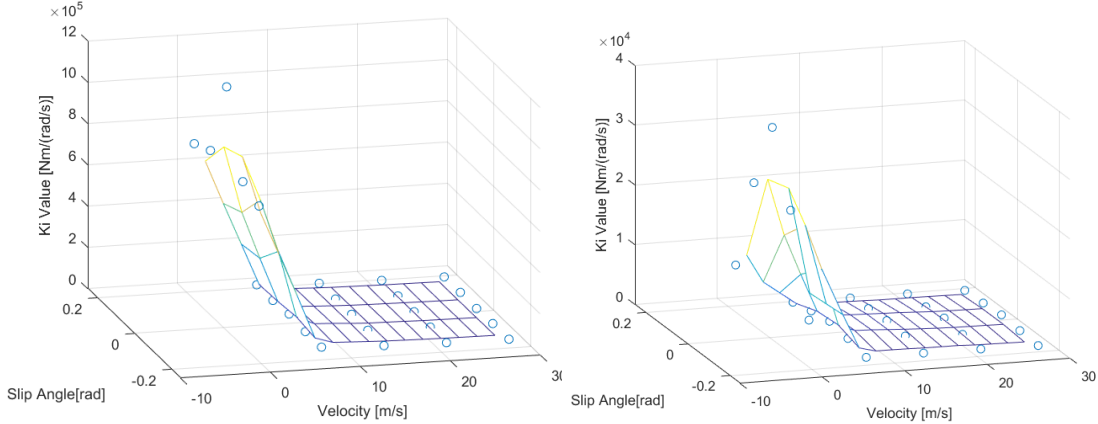

 Figure 5.2: K_p Plot

 Figure 5.3: K_i Plot

- A polynomial which depends on both scheduling variables:

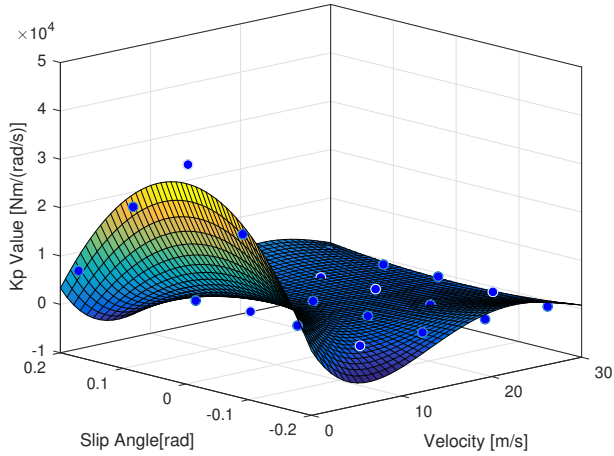
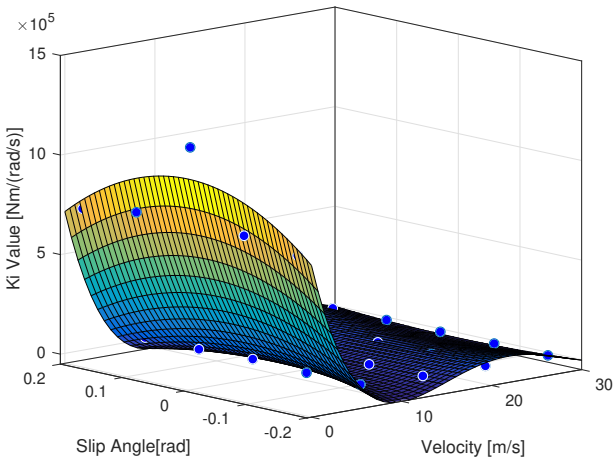
It might be a better approach to ensure a smoother transition between the constants for multiple working conditions. To generate the polynomial

$$K = p_{00} + p_{10}\alpha + p_{01}v + p_{20}\alpha^2 + p_{11}\alpha y + p_{02}v^2 + p_{30}\alpha^3 + p_{21}\alpha^2 v + p_{12}\alpha y^2 + p_{03}v^3 + p_{40}\alpha^4 + p_{31}\alpha^3 v + p_{22}\alpha^2 v^2 + p_{13}\alpha y^3,$$

the *Curve Fitting Toolbox* that MATLAB includes has been used, and the results are presented in Table 5.3 and Figures 5.4 and 5.5.

Table 5.3: Polynomial constants

Parameter	K_p Polynomial	K_i Polynomial
p_{00}	1.011×10^6	3.146×10^4
p_{10}	-2.294×10^5	-6006
p_{01}	6.134×10^{-9}	8.357×10^{-11}
p_{20}	1.824×10^4	432.9
p_{11}	-1.084×10^{-10}	$\times 10^{-12}$
p_{02}	-7.465×10^6	-7.029×10^5
p_{30}	-599.8	-13.73
p_{21}	-1.489×10^{-11}	-9.354×10^{-13}
p_{12}	7.528×10^5	6.805×10^4
p_{03}	-7.727×10^{-8}	-5.989×10^{-10}
p_{40}	6.95	0.1591
p_{31}	4.752×10^{-13}	2.16×10^{-14}
p_{22}	-1.617×10^4	-1439
p_{13}	5.675×10^{-10}	-3.159×10^{-11}


 Figure 5.4: K_p Polynomial - $R^2=0.968$

 Figure 5.5: K_i Polynomial - $R^2=0.968$

From Figures 5.4 and 5.5, it can be seen that a drawback of using a polynomial is that at high slip angles and low velocities, the value of the function gets negative. For this reason, during its implementation, it is quite important to establish a lower bound to ensure that the function always respects the minimum value.

By simulating with both options, it has been checked that both approaches would be suitable for the controller purposes. The one that has been used for simulations is the 2-Dimensional look-up table just because of its added simplicity.

5.4 Yaw Rate Controller Response

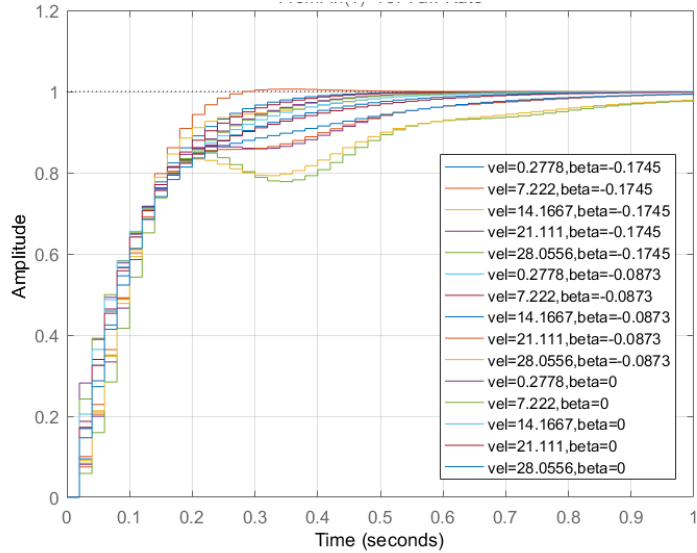


Figure 5.6: Step Response depending on operating condition

In Figure 5.6, the closed-loop step response for all the considered operating conditions is shown. Regarding this plot, there are some considerations to be mentioned.

- Firstly, the plot shows half of the operating conditions. That is because of the symmetrical response of the beta behaviour (with the same controller), meaning that, for example, the response between condition $\text{vel} = 14.1667 \text{ m/s}$, $\beta = -0.0873 \text{ rad}$ is the same as $\text{vel} = 14.1667 \text{ m/s}$, $\beta = 0.0873 \text{ rad}$.
- Secondly, although a lot of operating conditions are considered in the model linearization, there are some of them which are unlikely to happen, and those are the ones referring to high speed together with high slip angle (in fact, in this figure this situations are the ones that need more time to converge to steady state and have the less similar to a first-order response). This considered fact is because slip angle tends to get a higher value when the yaw rate is higher, and at high speeds this is a non-likely situation as the car would lose the grip and not reach the desired yaw rate.

When designing the controller, the frequency ranges of the input signal have been taken into account. By applying the Fourier Fast Transformation (FFT)[Smith, 1997] feature of the data analysis software (Section 3.7) have been used over the yaw rate signal shown in Figure 5.7. These data correspond to the Endurance event of Formula Student Spain.

In Figure 5.7, it is observable that the signal of interest exists approximately between a range $f \in [0.01, 1] \text{ Hz}$. That way, it is desired a high gain in this frequency range for the system to follow the reference with the least steady-state possible error.

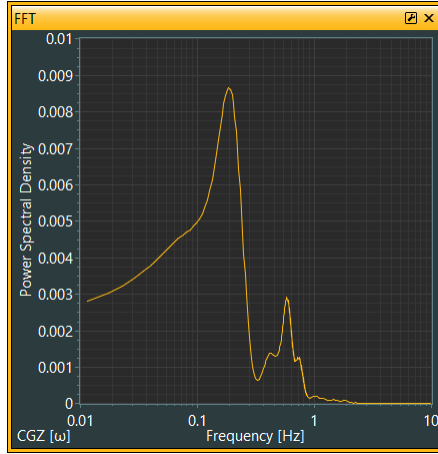


Figure 5.7: FFT Over Yaw Rate Signal

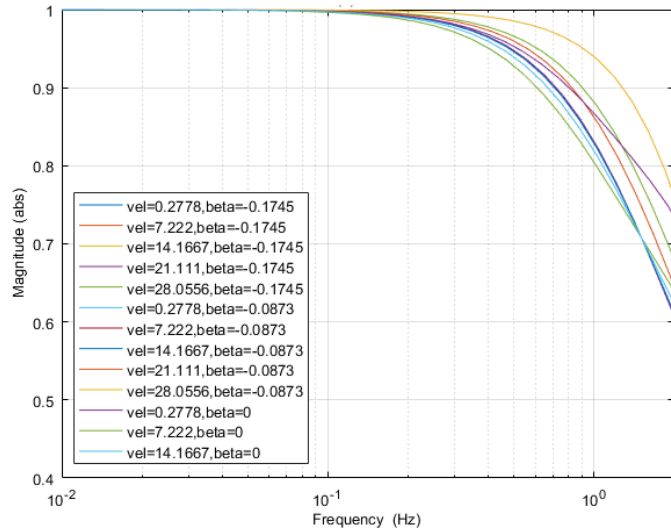


Figure 5.8: Closed Loop Bode Plot depending on operating condition

Although the designed Quasi-LPV model (4.1) approaches the behaviour of the vehicle with no large error, the parameters are possibly going to be tuned in real tests to improve the results and the controller response. As mentioned before, the plant to design the controller does not take into account the tire forces, for that reason the parameters values might be quite high. Also due to this fact, a feed-forward component to include the tire lateral forces might be included.

5.5 Feed-Forward Component

For the PI controller design, the considered plant has been $G(s) = \frac{\dot{\psi}(s)}{M_z(s)}$. However, this M_z is not in any case only generated by the longitudinal tire forces due to the motors output as the lateral forces also generate a considerable amount of $M_{z,Fy}$ because of the driver turning the

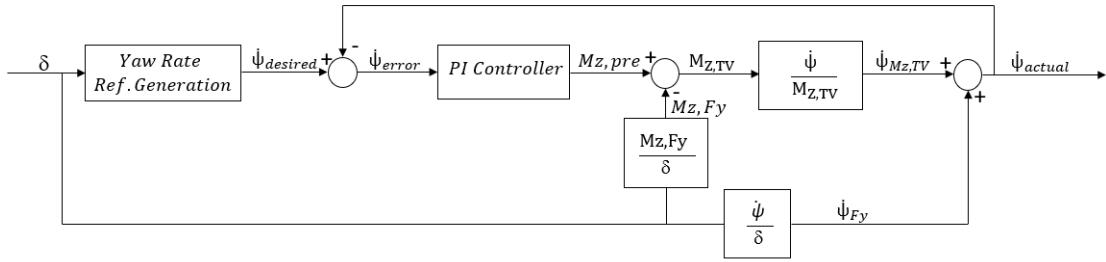


Figure 5.9: Feed-forward Scheme

steering wheel. For this reason, to determine the $M_{z,TV}$, a feed-forward component (Figure 5.9) may be included to take into account the lateral tire forces. As a result, it is possible to obtain the $M_{z,TV}$ as the target for the subsequent TD problem.

In this project, the CarMaker software from IPG Automotive⁴ is going to be used for simulations. Using that software is going to allow to substitute the $\frac{M_{z,Fy}}{\delta}$ for the M_z due to the longitudinal tire forces extracted from the CarMaker. For the implementation on the vehicle, as mentioned above, Kalman filters are going to be used.

As it also happens with the PI controller, the fact of including a feed-forward component may disturb the real behaviour of the controller, which is also a fact that may affect the parameter tuning process during real tests on track.

5.6 Anti-windup Component

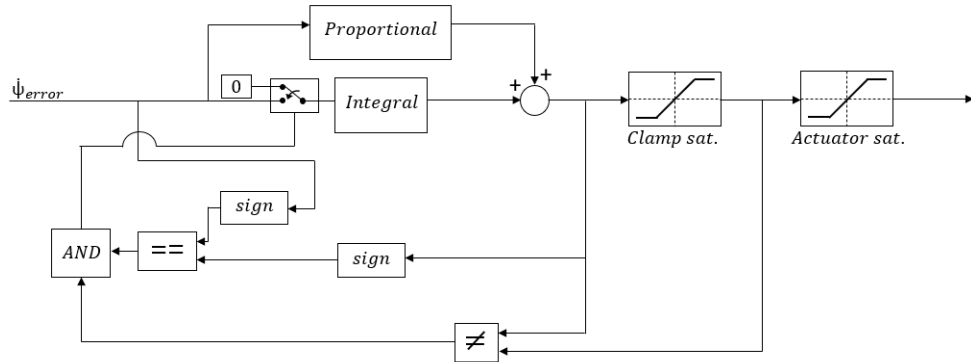


Figure 5.10: Anti-Windup Scheme

The objective of the anti-windup (Figure 5.10) is to let the whole control know when the actuators are saturating and by doing so, that the error must not be integrated. The anti-windup

⁴<https://ipg-automotive.com/products-services/simulation-software/carmaker/>

component may be necessary to avoid excessive and somehow erroneous integration of the yaw rate error. By including this component, the actuators limits are taken into account in case it would be necessary.

5.7 Summary

In this chapter, the first element of the control algorithm, the yaw rate controller, has been presented together with the generation of its input ($\dot{\psi}^{ref}$) coming from the intentions of the driver. The importance of this controller relies on the fact that its output is one of the signals for the TD problem (Section 6.3), necessary to fulfil the driving requests. Lastly, the results of the controller response have been discussed together with the components that surround it, which are the feed-forward and the anti-windup have been discussed.

Once the yaw rate controller has been designed and all the reference signals for the last element of the TV are defined, the design of TD multi-objective optimization problem can be realized as presented in the Chapter 6.

Chapter 6

Torque Distribution Problem

6.1 Introduction to Torque Vectoring

Torque Vectoring is a technology which main objective is to distribute the instantaneous power (in terms of torque) developed by the vehicle among the four actuators with the objective of optimizing this distribution process. There are different approaches to a TD problem, mostly depending on the power-train configuration used (e.g., number of motors, existence or not of differential or position of the motors). In general terms, this algorithm can include the following objectives:

- **Safety:**

It can prioritize the stability of a vehicle. In road cars, for example, it can be useful in case of fast lane changing by enabling the car to turn as fast as possible working under certain grip limitations and maximize stability.

- **Maneuverability:**

It can be useful for turning the car faster, with less effort or even enabling to turn with a smaller turning radius.

- **Traction and Performance Improvement:**

By sending the torque to where it is more adequate, it can make the wheels work constantly over optimal values for slip ratio maximizing the available longitudinal force together with traction either in a race track, for race vehicles, or on the countryside with irregular terrains for all-terrain vehicles. By working over the mentioned optimal slip ratio range, waste of the rubber of the tires can also be considerably reduced.

- **Energy Optimization:**

By using the least energy possible to fulfil the driver commands while taking into account the vehicle dynamic limitations without over-passing them, which is also a way of distributing energy in a more efficient way.

In this project, the principal objectives are traction and performance improvement to reduce time per lap. However, safety, maneuverability and energy optimization are, although with lower priority, also included.

The aim of the proposed algorithm is to satisfy the desired yaw rate (which is proportional to referring to M_z^{ref}) and longitudinal acceleration (which is proportional to referring to F_x^{ref}) in cornering and straight track sectors respectively. This M_z and F_x references are going to be continuously considered to be followed with the help of the TD solution.

To accomplish the mentioned objectives, the stated problem is going to focus on the tire force distribution. Tires have their corresponding circle of friction (Section 3.4.1), and it is going to be considered at all instants to determine the optimal longitudinal force that tires can handle and by consequence, the corresponding torques.

6.2 Torque Distribution Control-Oriented Model

Firstly, it is important to describe F_x and M_z expressions in terms of the algorithm output signals, wheel torques, as follows¹:

$$F_x = \frac{1}{R_w} (\cos(\delta_1) \Gamma_1 + \cos(\delta_2) \Gamma_2 + \Gamma_3 + \Gamma_4), \quad (6.1a)$$

$$M_z = - \left(\sin(\delta_1) l_f - \cos(\delta_1) \frac{t_f}{2} \right) \frac{\Gamma_1}{R_w} + \left(\sin(\delta_2) l_f - \cos(\delta_2) \frac{t_f}{2} \right) \frac{\Gamma_2}{R_w} - \frac{t_r}{2} \frac{\Gamma_3}{R_w} + \frac{t_r}{2} \frac{\Gamma_4}{R_w}, \quad (6.1b)$$

where Γ_i [Nm] is the torque of each wheel, δ_i [rad] is the steering angle for the front tires, t_f [m] is the track of the front axis and t_r [m] is the track of the rear axis.

If small slip angles were considered, $\sin(\delta) = 0$ and by $\cos(\delta) = 1$, and applying this simplifications over (6.1), it yields

$$F_x = \frac{1}{R_w} (\Gamma_1 + \Gamma_2 + \Gamma_3 + \Gamma_4), \quad (6.2a)$$

$$M_z = - \frac{t_f}{2} \frac{\Gamma_1}{R_w} + \frac{t_f}{2} \frac{\Gamma_2}{R_w} - \frac{t_r}{2} \frac{\Gamma_3}{R_w} + \frac{t_r}{2} \frac{\Gamma_4}{R_w}. \quad (6.2b)$$

In this project, no simplifications for slip angles are made, so small slip angles are considered and the whole algorithm is created around (6.1).

6.3 Torque Distribution Optimization Problem

In CAT13e, four completely independent electrical machines are responsible of the power-train actuation, which means that these actuators have to work together, in harmony, in order to avoid a possible unsafely behaviour of the vehicle. The TD problem is in charge of considering the driver desires together with the vehicle dynamic limitations to ensure safety while

¹Equations (6.1) are extracted from Figure 3.4 in Section 3.4. Also notice that self aligning torques are neglected as they are quite difficult to determine and their value is not as significant es the one resulting either from the longitudinal or lateral forces of the tires.

maximizing the performance of the vehicle.

The main idea behind the TD problem is to be able to find the optimal outputs, which are the four correspondent torques, taking constantly into account the dynamic limitations of the vehicle. To have these limitations into account, the algorithm is continuously fed by the working point of the tire to determine the most adequate way to distribute the power to fulfil the driving intentions while maximizing the performance. The multi-objective optimization problem is presented as follows:

$$\min_{\Gamma} \sum_{m=1}^3 \alpha_m J_m \quad (6.3a)$$

$$\text{subject to} \quad (6.3b)$$

$$\Gamma_i \in [\Gamma_{min}, \Gamma_{max}], \quad \Gamma_i \subseteq \mathbb{R} \quad \forall i = 1, \dots, 4 \quad (6.3c)$$

$$F_x \in [F_{x,min}, F_{x,max}], \quad F_x \subseteq \mathbb{R} \quad (6.3d)$$

$$M_z \in [M_{z,min}, M_{z,max}], \quad M_z \subseteq \mathbb{R} \quad (6.3e)$$

$$\sum_{i=1}^4 \eta_i \Gamma_i \omega_i \leq P_{max}, \quad P_{max} \subseteq \mathbb{R} \quad (6.3f)$$

where² α_m are the priority factors for the proposed objectives J_m , F_x [N] is the instantaneous longitudinal force determined by (6.1a), M_z [Nm] is the instantaneous momentum determined by (6.1b) around the Z axis of the vehicle, $F_{x,min}$ [N] and $F_{x,max}$ [N] are the bounds for the longitudinal force, limited by the friction circle of the tires at every instant, $M_{z,min}$ [Nm] and $M_{z,max}$ [Nm] are the bounds for the yaw momentum, also limited by the friction circle of the tires at every instant, η_i is the efficiency corresponding to each motor due to losses in itself and between the connection to the battery, ω_i [rad/s] is the speed of each wheel and P_{max} [W] is the maximum allowable power due to competition rules. Once the problem is stated, its different objectives are defined. Starting with the optimization problem, it consists of three differentiated objectives outlined below.

The first objective J_1 corresponds to the error between the longitudinal force desired by the driver and the force due to the instantaneous developed torques. This objective can be expressed as

$$J_1 = \|F_x - F_x^{ref}\|^2, \quad (6.4)$$

where F_x^{ref} [N] is the desired longitudinal force that the driver desires.

Although (6.4) is not considered the most important objective (justification in Section 7.2), it must be taken into account to considerably improve the feelings of the driver while accelerating, which leads to a better performance.

The second term of (6.3a) is referred to the error between the desired yaw moment, the output signal of the yaw rate controller, and the instantaneous yaw moment due to the torque developed by the motors, i.e.,

²Notice that F_x and M_z are determined by (6.1).

$$J_2 = \|M_z - M_z^{ref}\|^2, \quad (6.5)$$

where M_z^{ref} [Nm] is the desired momentum, which is the output of the yaw rate controller.

The main aim of the TV is to improve and optimize the behaviour while cornering, so this second term is clue in the achievement of the desired results.

The last term of (6.3a) is referred to the value of the torques themselves and allows to regulate the amount of torque to achieve the first and second objectives of the optimization problem. The involved expression can be written as

$$J_3 = \|\tau\|_{\alpha_3}^2. \quad (6.6)$$

Here, J_3 is a quite interesting component as it also indirectly allows to select the static amount of power that is sent to each front and rear axle. It is important to notice that the weighing factor α_3 is presented in this case. The reason is because this third priority factor is not an scalar (while it is the case for α_1 and α_2) but a diagonal matrix of dimension 4×4 because a term for each one of the torques is needed to determine the previously mentioned power to each axle. Analyzing (6.1b), if t_f is larger than t_r , which is the case for the CAT13e, the algorithm is going to apply more torque to the front axle as more M_z is reached with lower values for those front torques in comparison with the rear ones. However, because of weigh distribution and load transfer while accelerating, the selected static priority determines that the car must prioritize sending torque to the rear axle.

In this project, the most important objective of the TD problem is to prioritize the minimization of the yaw moment error while considering the possibility to reduce the energy needed to minimize also the time per lap. To achieve those objectives, multiple priority factors for the proposed objectives in (6.3a) (α_1 , α_2 and α_3) have been tested between a given range of values to finally simulate the resultant combinations and discuss the consequent results in Section 7.2.

Regarding the four constraints in (6.3), three of them are given due to vehicle dynamic limitations and the last one is due to the rules of the Formula Student competition. All these restrictions are discussed next:

- Constraint (6.3c) refers to the minimum (which, in this case, is equal to 0, as no regenerative braking is considered) and maximum value of the torque that can be sent to a determined wheel. Referring to this second mentioned term, the maximum value, it is important to notice that it is an input for the TD problem itself, as they purely depend on the instantaneous point where the tire is working inside the friction circle (Section 3.4.1).
- Constraints (6.3d) and (6.3e) are also completely dependent on the circle of friction, which determines the two low and high limits for F_x and M_z by applying the instantaneous maximum values of the torques into (6.1).

- Finally, the constraint (6.3f) refers to the developed power. Formula Student Rules establish that the maximum developed power of a vehicle must be 80kW in any competition event. That rule has to be taken into account not to be penalized and it can be perfectly included in the algorithm. The only drawback is that to apply this restriction in this algorithm, is that it must be a function of $\Gamma_i \forall i$, which force to have a well-studied efficiency map of the electrical machines in order to gain precision and get as close as possible to the maximum allowed torque without over-passing it.

6.4 Summary

In this chapter, the different approaches for the TV algorithm have been discussed, together with the expected objectives to achieve with its implementation in the case of this project.

Once the general objectives were exposed, the last component of the TV, the TD, has been presented. The multi-objective optimization problem (6.3) that forms this algorithm has been discussed together with a detailed explanation of each of its three sub-objectives (6.4), (6.5) and (6.6) and the constraints that govern them (6.3c), (6.3d), (6.3e) and (6.3f).

At this point, the elements that conform the TV have all been presented. The yaw rate controller (Chapter 5) together with its model (4.1) and the TD multi-objective optimization problem (Section 6.3) have been assembled in MATLAB/Simulink inside the IPG-CarMaker environment to obtain the results presented in Chapter 7.

Chapter 7

Torque Vectoring Simulation and Results

7.1 Introduction to simulation and results

Throughout this project, all the steps to get to an optimal distribution of the power over the four power-train actuators of CAT13e have been discussed.

The topic of interest, which have been the content of this project until this point have been the yaw rate controller in Chapter 5, the Quasi-LPV model used to design the controller, in Chapter 4 and the TD optimization problem in Section 6.3. Once all the TV components have been presented, it is going to proceed with the results obtained from their assembly.

In this chapter, the results of all the assembled control modules are going to be presented and discussed. Starting from finding the most properly calibrated TD problem based on two Key Performance Indicators (KPIs) and analysing its results. With the selected priority values (α_1 , α_2 and α_3), the results of the TV are going to be presented and discussed. These data shown in the results have all been obtained from the IPG-CarMaker software (Figure 7.1).

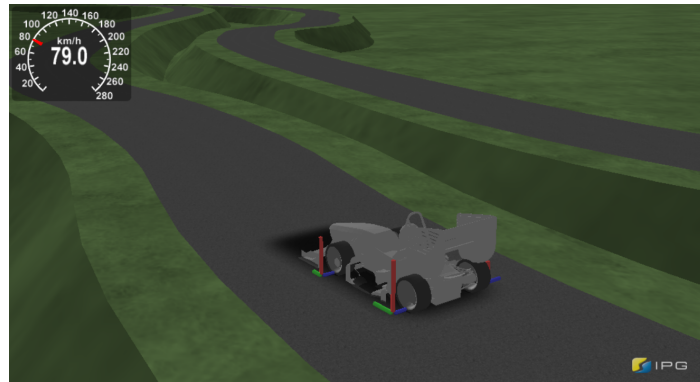


Figure 7.1: IPG Simulation Example

7.2 Torque Distribution

To find a solution to the TD problem (Section 6.3) at each sampling time, a Quadratic Programming (QP) solving process has been applied by using the CPLEX solver from the *IBM Corporation* company (a software which they lend for free to student users). This solver is used inside the MATLAB/Simulink environment together with the *Interpreted MATLAB Function* that Simulink offers in order not to generate the C-Code for the CPLEX algorithm but run it inside the same environment.

As previously presented in Section 6.3, there are three distinguished objectives for the TD problem. In order to analyze the most adequate priority for each of them, multiple lap simulations have been performed to compare such objectives and decide the best combination based on two Key Performance Indicators (KPIs). These indicators are the *Lap Time* and the *Energy Consumption* during one lap.

Table 7.1: Influence of the prioritized objectives

Objectives Weights [%]		Lap Time [s]	Energy [Wh]
$\tau = 10\%$	$M_{z,err}=50\% \quad F_{x,err}=40\%$	59.06	267.31
	$M_{z,err}=60\% \quad F_{x,err}=30\%$	59.08	272.32
	$M_{z,err}=70\% \quad F_{x,err}=20\%$	58.55	280.32
	$M_{z,err}=80\% \quad F_{x,err}=10\%$	58.95	272.05
$\tau = 20\%$	$M_{z,err}=50\% \quad F_{x,err}=30\%$	58.65	268.65
	$M_{z,err}=60\% \quad F_{x,err}=20\%$	58.28	276.37
	$M_{z,err}=70\% \quad F_{x,err}=10\%$	58.94	266.71

Regarding the computation of the considered KPIs, the energy is calculated as

$$E = \sum_{n=1}^4 \int_0^{t_s} \eta_i \Gamma_i \omega_i dt,$$

where t_s is the lap time [s] and n refers to each one of the wheels. However, when implemented on the CAT13e, it is going to be measured by an *Isabellenhütte IVT-MODular* sensor which calculates the energy consumption as

$$E = \int_0^{t_s} V_b I_b dt,$$

where V_b is the instantaneous voltage of the energy accumulator (or battery) [V] and I_b is the output current of the energy accumulator [A].

From Table 7.1, some interesting conclusions can be drawn. Referring to the first KPI, it is observable that neither prioritising the M_z nor the F_x significantly improve the results, but around a 65-25% relation between them is the best option in terms of reducing lap time. Also from this analysis, it can be determined that, although not being the best option, maximising the M_z would be better than doing so with the F_x . The better results of maximizing M_z over F_x is because, maximizing M_z , the desired yaw rate by the driver is better acquired, which

reduces time though curves together with the time needed to get ready for the following curve or straight with less time needed. However, it would have an important drawback, which is that the driver could feel that the car does not accelerate exactly as he/she wants during a curve exit as F_x is not much relevant.

Secondly, referring to energy consumption, although there are no significant differences, it must be taken into account that, for example, for an Endurance Event, the vehicle must complete 20-22 laps. The amount of laps mean that a difference of 15Wh in one lap leads to approximately 300Wh (which is near a 5% of the total battery capacity) in an Endurance Event. Acquiring more data during testing about more precise results could mean reducing the battery capacity, leading also to a weight reduction.

Finally, the J_3 component of (6.3a) and its priority factor value are discussed. At first sight, it could be said that neither giving more nor less priority to J_3 affects energy consumption of the vehicle in a significant way. However, analysing at the same time both KPIs, it is remarkable that, with the same amount of energy, lap time becomes reduced with a higher priority to J_3 . That could seem strange, but the J_3 component of the TD problem is really interesting because it not only allows to *limit* the power to achieve the objective, but it also allows to control the amount of power that the front and rear axles may develop in terms of percentage distribution between them.

That apparently not much significant consideration is really an important fact to take into account. Nearly all sport and racing cars are rear wheel drive, normally due to its weight distribution and the gain in vertical load at the rear axle while accelerating, and what the inclusion of J_3 implicitly mean is that, correctly calibrated, it can make a car predefined to behave similarly as a rear wheel drive car, and maximize the use of the front motors when the rear axle is saturated and cannot achieve the objectives by its own.

The last consideration of this third component of the TD problem, is that as the percentage of power to the front and rear axle can be controlled, it allows to reduce the power difference developed by both axis. The possibility to control that power difference could be useful to stabilize the temperature electrical machines as they work over nominal conditions quite often and tend to rapidly increase their temperature, which may lead to ask the driver to decrease the pace.

CPLEX Solver considerations

For the implementation of the algorithm into the main ECU of the CAT13e (which sample time is 20ms, and for that reason that time is the one used for simulations), it is important to have constantly monitored the *Exitflag* variable output of the CPLEX Solver, which refers to the feasibility and optimality of the result.

This variable is important because in case the TD problem is infeasible or a solution is not found in a determined instant, a safe reference for the electrical machines to follow must be



sent in order to maximize security. To do so, an option would be maintaining the result of the previous iteration during more than one sample. Whether for some reason the behaviour of the exitflag was not as desired, it could also be considered to switch off the algorithm and maximize safety and the opportunities to finish the competition event.

7.3 Analysis of the vehicle behaviour

Given the results achieved in Section 7.2, to present the following results, it has been selected the weights of: $M_{z,err} = 60\%$, $F_{x,err} = 20\%$ and $\tau = 20\%$. All the simulations have been around the FSS Endurance circuit presented in Figure 4.4, except the comparison between the TV active and disabled, which comparison has been made over a Skidpad test for simplification.

7.3.1 Yaw Rate Controller

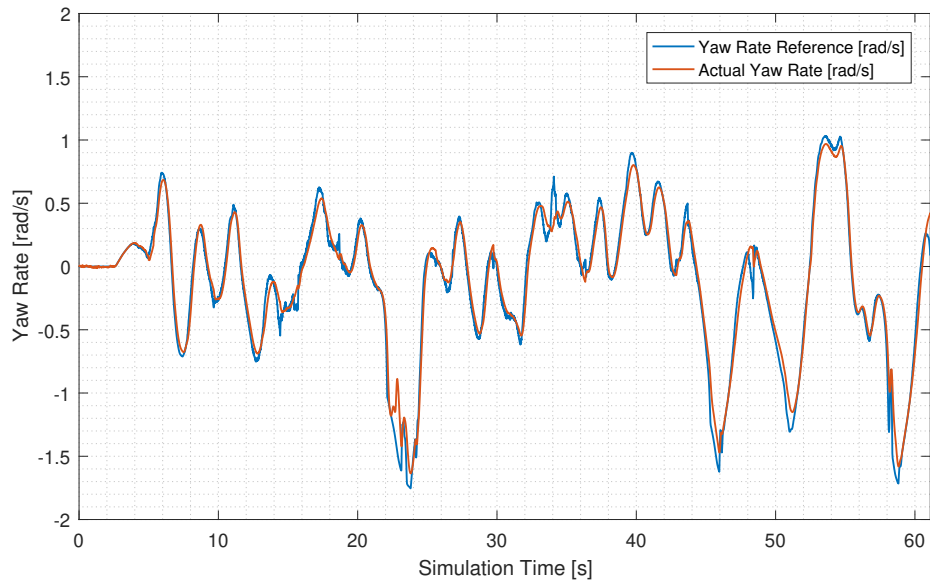
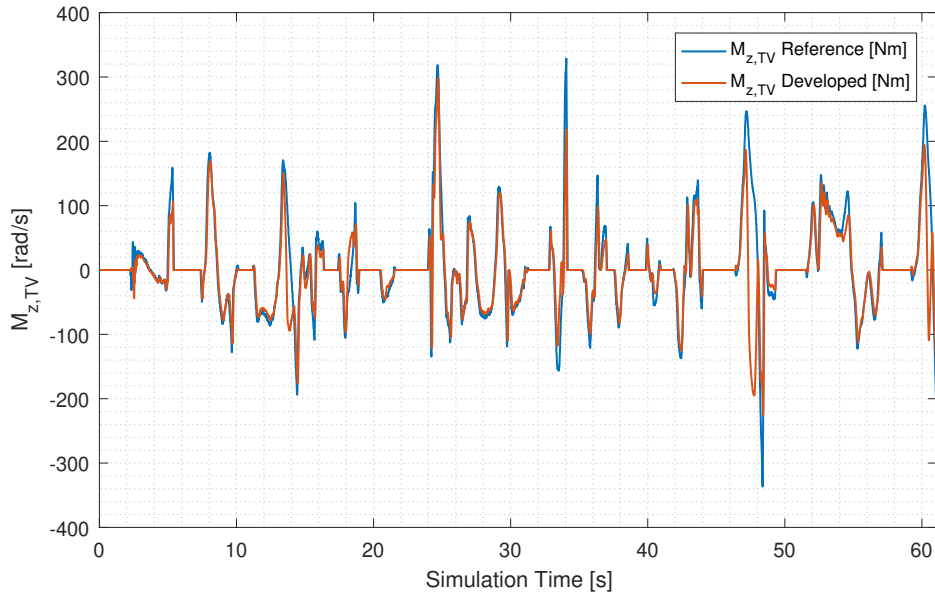


Figure 7.2: Yaw Rate Response

In Figure 7.2, the *Yaw Rate Reference* and the *Actual Yaw Rate* signals are plotted. The reference corresponds to the result of applying (5.3) over the driver input δ with a selected $K_u = -0.0005$ ¹. An important observation that must be done is that the yaw rate limit (5.5) is also considered here, limiting, for example, the reference between $t=22s$ and $t=23.7s$. Moreover, the actual yaw rate is the result of the forces of the tires for both lateral and lon-

¹Just as a notification, it is observable that there are few peaks that look surprising around $t=36.5s$ and $t=48.5s$. These remarks are due to some unexpected peaks in the driver steering angle which depends on how the driver is programmed inside the IPG-CarMaker.


 Figure 7.3: $M_{z,TV}$ Response

itudinal forces (the ones controlled by the TV).

From the obtained results, it is shown that the car follows the reference quite faithfully, what leads to conclude that the yaw rate controller is quite correctly tuned, although, as previously mentioned, some parameters may be tuned during tests on track with the CAT13e.

7.3.2 Desired M_z vs Developed M_z

In Figure 7.3 the $M_{z,TV}$ Reference and the Developed M_z are compared. The first one corresponds to the output of the yaw rate controller (Section 5), and the second one corresponds to the generated moment due to the TD outputs (Section 6.3). Regarding to the yaw rate controller, the one used during simulations has been a proportional one for two reasons:

- The vehicle does not reach a stationary state at any time frame.
- During the CAT12e tests on track, the feedback from the drivers was that, with the integral component, the car was less intuitive to drive, so they did not feel as confident as with only the proportional one. As previously mentioned in Section 3.7, the feedback of the drivers is quite important, so in this case it is been considered to take it into account.

In the obtained results, it can be drawn that the four torques are generating an adequate yaw moment which has quite a suitable behaviour following the reference yaw moment signal, what leads to conclude that the torques are correctly distributed obtaining the desired results.

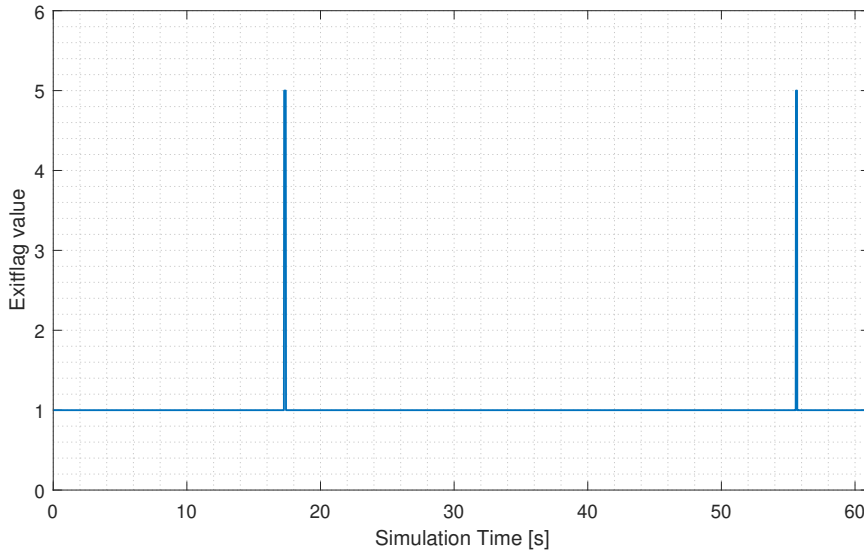


Figure 7.4: Exitflag Value

At this point, it is important to analyze also the *exitflag* behaviour, to determine whether it has a suitable value during simulations as presented in Figure 7.4. The possible exitflag values are presented as follows:

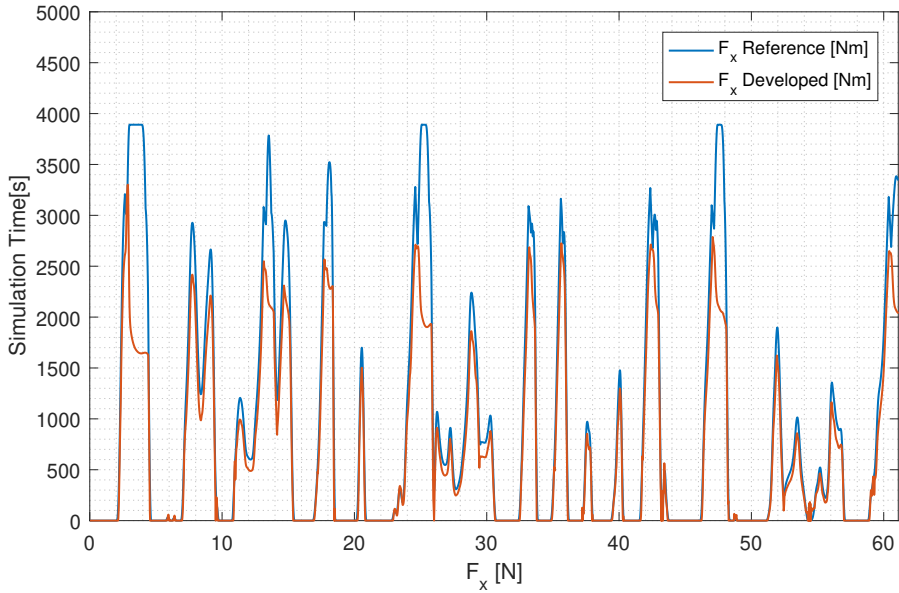
- 0: Number of iterations exceeded.
- 1: Function converged to a solution x.
- 2: No feasible point was found.
- 3 Problem is unbounded.
- 4: NaN value was encountered during execution of the algorithm.
- 5: Both primal and dual problems are infeasible.
- 7: Search direction became too small. No further progress could be made.

In Figure 7.4 it is shown that the CPLEX solver converges to a solution during nearly the whole simulation except in two short time frames in which the problem is infeasible. During this instants, one previously commented solution could be maintaining the last value corresponding to a feasible solution. The behaviour of this variable must be studied when implemented on the CAT13e before the activation of the TV for the first time for safety reasons.

7.3.3 Desired F_x vs Developed F_x

In Figure 7.5, the *Reference F_x* and the *Developed F_x* are shown. The first one corresponds to the longitudinal force that the driver requests through the accelerator pedal and the second one is the result of the output torques of the TD problem. It is important to remark here that




 Figure 7.5: F_x Response

F_x has less priority than M_z when minimizing their error with respect to their corresponding reference. However, the resulting difference is not much significant above a requested value of $F_x = 2500$ N (which corresponds to an acceleration of around 1g)².

By the results obtained, it can be concluded that the car accelerates as the driver intends to and only at some points it accelerates a little bit less as a result of tires saturation and also the preference to follow the M_z . However, both signals, *Reference F_x* and *Developed F_x* , have the same profile and the results are considered suitable.

7.3.4 Torques

In Figure 7.6, the developed wheel torques, which are the output of the TD optimization problem, are shown. The corresponding motor torques are the plotted values divided by the transmission relation. From this figure, some interesting conclusions can be drawn.

One of the objectives during the TD problem design was to distribute the power between the front and rear axles in a way that they led the car to behave similar to a rear wheel drive vehicle. Having remarked that, and regarding Figure 7.6, it is noticeable that during the whole lap, the torque developed by the front motors is higher than the torque developed by the rear ones (just as a notification, this comparison must be made by analysing right and left side electrical machines independently, not to consider the generated M_z as a variable in this sub-analysis).

²At this point, it is important just to mention that the feeling of the driver is going to be important during its implementation on the CAT13e.

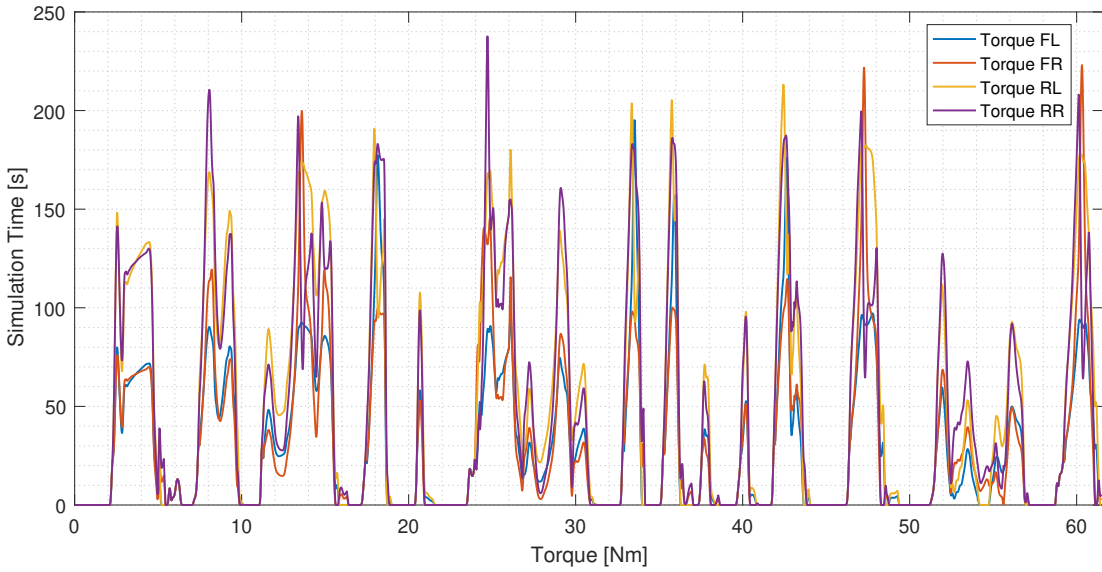


Figure 7.6: Wheel Torques

A consequence of the observation above is that, although more power is sent to the rear axle, the four motors are developing a considerable amount of power. This power distribution is interesting as it causes that none of the motors work excessively over nominal conditions, which leads to less power losses (as the efficiency of the motors decrease together with the increase of developed power) and as a consequence, the motors tend to over-temperature less, what may avoid having to decrease the pace due to temperature issues.

Finally, it is wanted to be remarked that the distribution shown in Figure 7.6 is because of the selected priority for each one of the objectives of the TD problem. An interesting point is that this distribution is quite versatile and can be either adapted to the driver behaviour or optimized for each one of the competition events (Chapter 2).

7.3.5 Power Limitation

In the Formula Student competition, a vehicle must not develop a power over 80kW during any of the four dynamic events (it is established in the Formula Student Rules 2020³, Section EV 2.2.1).

There are different ways to follow that rule, but in this project it has been decided to include the power limitation as a restriction in the TD problem as the constraint (6.3f). In Figure 7.7, the difference between the data corresponding to the simulation where the limitation is respected and the one where there is no power restriction taken into account is shown.

³<https://www.formulastudent.de/fsg/rules>.

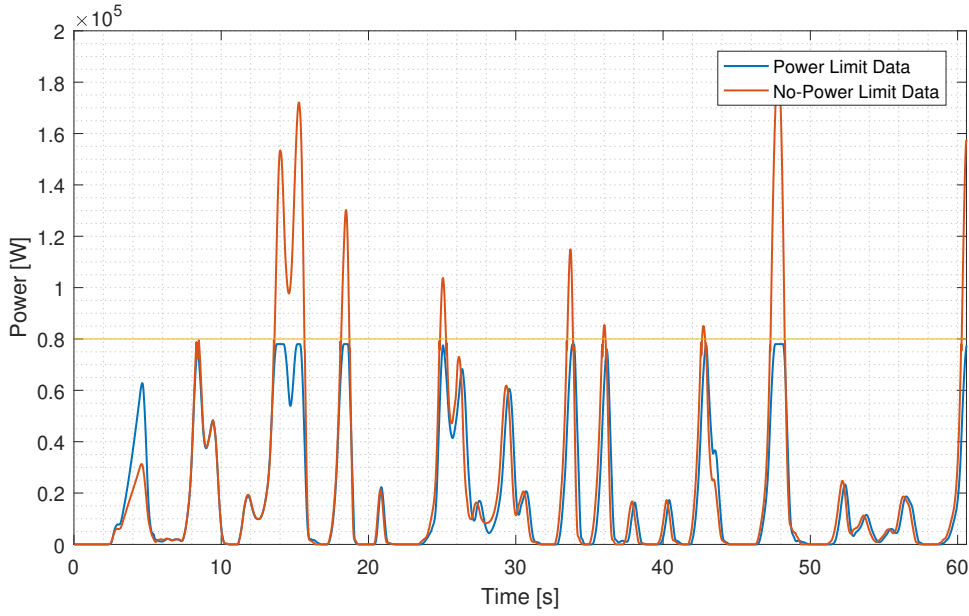


Figure 7.7: Power Limit Behaviour

In Figure 7.7, it is noticeable how the algorithm which includes the power limitation maintains the power below 80kW (a safety margin of 2kW had been established and limit was set at 78 kW), while if the algorithm does not take into account that power, the vehicle surpasses 80kW. An interesting observation is that, in order not to exceed the power limit, the limitation should be slightly below the maximum allowed value. This is because, due to the sampling time in which the calculus are made, a little overshoot could appear, and if it reaches a value over 80kW, a penalty would be applied to the team in a determined event.

Finally, regarding the power, it is observable how the lap time is reduced in some tenths of a second in the case in which the power limitation is not considered.

7.3.6 Torque Vectoring Active vs Torque Vectoring Disabled (25% Distribution)

To compare the results between a simulation with TV and another with a distribution of the torque correspondent to 25% of the torque to each electrical machine, the simulation has been made over a Skidpad test.

In Table 7.2 the results obtained from two Skidpad test runs are compared. As shown in this table, when the TV is active, the results improve quite considerably. Regarding the average yaw rate, it increases 0.1 rad/s (Figure 7.8) when the TV is active, which is an 8.4% increase in comparison with the run with a torque distribution of 25% to each motor. This improvement allows the vehicle to reduce the Skidpad time in 0.375s, which is a quite considerable improvement.

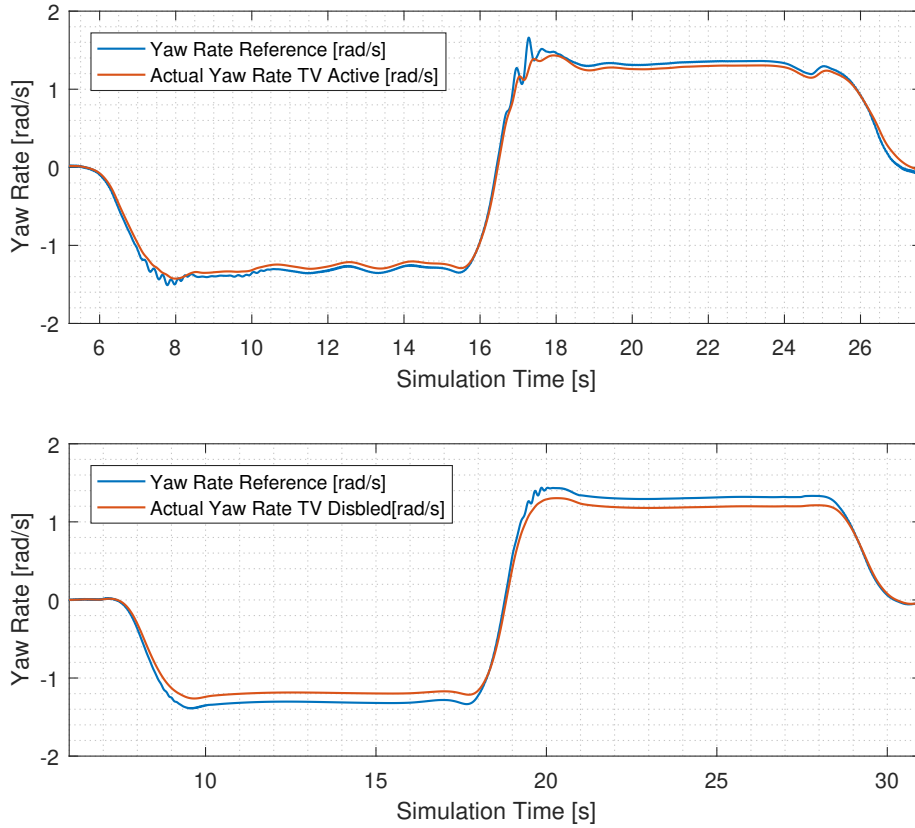


Figure 7.8: Skidpad Comparison

Table 7.2: Skidpad Comparison

Variable	TV Active	TV Disabled
Peak Yaw Rate	1.43	1.3
Yaw Rate Average	1.29	1.19
Left Turn Time	4.84	5.24
Right Turn Time	4.85	5.2
Total Time	4.845	5.22

Analysing the obtained results, it can be concluded that the TV algorithm is suitable and worth being included in a vehicle like the CAT13e with four in-wheel independent electrical machines.

7.4 Summary

In this chapter, all the results of the TV designed in this project have been shown and discussed, focusing on the overall behaviour of the vehicle. Together with the conclusions of the

consequent behaviour resulting of the TV control system inclusion, a comparison between including this control system, and not doing so, has been presented, which allowed to determine the benefits of implementing the presented work.

Chapter 8

Economical Analysis

In this section, a resumed brake down of the cost of this project is presented. The considered costs are approximate and variable. An important consideration is that these costs are reduced a 96.65% due to the fact that all the engineers, together with the author of this project, involved in *testing preparation* and *testing* are bachelor or university master students which take part of this project with the aim of learning. The other important consideration is that the software used was lend for free by project sponsors or companies that borrow free licences to students.

Table 8.1: Costs table for involved tasks

Task	Hours	Engineers	Cost [€/h]	Cost [€]	Real Cost [€]
Testing Preparation	12	6	90	1080	0
Testing	40	8	140	5.600	100
Data Analysis	50	1	15	750	0
Model Design	30	1	15	450	0
Model Validation	25	1	15	375	0
Controller Design	20	1	15	300	0
Torque Distr. Design	30	1	15	450	0
TV Validation	80	1	15	1200	0
Total	287	-	-	10.205	100

Table 8.2: Costs table for involved resources

Resource	Cost [€]	Real Cost [€]
Computer	250	250
DataAnalysisPro License	350	0
Matlab License	1800	0
CPLEX Solver	597	0
Microsoft Office Software	600	0
Total	3597	250

Chapter 9

Environmental impact

There are many studies [Lutsey and Hall, 2018] which determine that electric vehicles have much less environmental impact than petrol vehicles. Nowadays, an electric vehicle is around 30% cleaner than an internal combustion engine vehicle in terms of energy consumption and a 100% in terms of gas emissions. A part from that, electrical mobility is a constantly-growing part of the industry, and there are intense efforts to use less-damaging elements for battery packages and also improving its capacity to being recycled.

The study topics covered in this project do not allow to extract conclusions that could lead to having a great effect over the environment. However, there are two interesting points that are worth commenting on, and are presented next:

- Energy management:

Regarding the consumption of energy, it has been determined that in approximately 22km, a vehicle could save around 300 Wh. This value is considered quite remarkable as it means that a vehicle becomes around a 4.5% more efficient while improving its performance with the implementation of the TV. Another interesting consideration regarding this point, is that including the regenerative braking, the efficiency percentage may become considerably increased.

- Tire ware:

Regarding the tire ware, it has also been presented that it is reduced with the implementation of the TV as the undesired wheel spinning is less-likely to happen, as the control algorithm does not send power to a motor that cannot handle it. With more data, concrete numbers will be able to be presented in terms of the distance that a set of tires are going to cover before excessive degradation. It is important to be remarked, as tires have a considerable environmental impact in terms of energy consumption and CO₂ footprint to be manufactured.

This page is intentionally left blank.

Chapter 10

Conclusions & Further Work

The main objective of this project was to develop a Torque Vectoring (TV) control system algorithm from scratch to its final results. Due to the circumstances, implementation and results over the CAT13e vehicle have not been possible to carry through, but simulation results have been satisfactory and encouraging for a further implementation of the proposed control algorithm in this project. In this section, the achieved objectives and the further work are presented.

Main Contributions

From an overall point of view, the contributions of this project that are going to be useful for further improvements inside the ETSEIB MotorSport Formula Student team are outlined next:

- A Quasi-LPV bicycle model whose code has been created to be further modified in case the vehicle or tire properties vary in new prototypes of the team.
- A gain scheduling-based yaw rate controller which has been kept as simple as possible to reduce the possible sources of problems in the whole control algorithm. The proposed approach is to firstly validate the Torque Distribution (TD) with a reference coming from a relatively non-complex controller and improve this controller once the TD validation has been finished.
- A TD problem to ensure a proper power distribution over the multiple power-train actuators of the vehicle. The code for this algorithm has been created in a way that the priority parameters can be tuned in case it is needed for the purposes of the person in charge of this task during another Formula Student season.
- A TV algorithm which is the assembly of both the yaw rate controller and the TD problem.

What has been done

- An analysis of data focusing on obtaining results for further control purposes has been performed. Some vehicle dynamics have been explained, to favor further assumptions understanding, and those explanations have been complemented and discussed with the support of the analyzed data obtained during tests on track with the vehicle of last season, the CAT12e. Using the DataAnalysisPro software together with MATLAB have been essential to achieve the results and create visual support, such as figures or tables, to get the resultant conclusions.
- Some of the obtained results from the analysis of the data have been subsequently used to create the control-oriented Quasi-LPV model (4.1). Regarding that model, its definition and statement have been realized in order to accurate the behaviour of the yaw rate controller. Regarding the self-developed model (4.1), it was firstly purposed to analyze the improvement it could mean in terms of modelling the real behaviour of the car. After the statement and validation of this model, it has been determined that including the vehicle sensitivity in a simple bicycle model improves the results a considerable 20%, which allows to design a more accurate yaw rate controller.
- With the Quasi-LPV model (4.1), a set of yaw rate PI controllers has been designed. The controllers constants have been chosen taking into account the two scheduling variables in (4.1). By doing so, the objective of controlling a non-linear system, which is the vehicle, by using linear controllers has been fulfilled. Just as a remark, it had been considered important to ensure a smooth transition between the multiple working conditions of the controller, so a surface for each controller constants (K_p and K_i) has also been implemented.
- With the yaw rate controller tuned to accomplish the desired control objectives, the inputs for the TD algorithm were nearly completed. The only work left, which also has been done, was to determine the maximum torques that each motor could develop. To do so, the friction circle obtained during the data analysis process has been crucial to include the tire behaviour inside the TD problem.
- With all the needed inputs, the TD multi-objective problem has been created. The equations and restrictions have been selected in order fulfill the desired vehicle behaviour and all the results have been presented to support the consequent improvements of the implementation of the TV into a car with multiple electrical machines.
- An important task has been preparing the MATLAB/Simulink environment to work together with the IPG CarMaker software. Also, including the functionality of the CPLEX solver has been crucial at this point to be able to obtain proceed with the simulations. Finally, an analysis of data extracted from simulations has been presented and discussed. From this analysis, it has been concluded that the implementation of a TV control system is considerably beneficial for a vehicle with multiple electrical machines for the following reasons:
 - Vehicle versatility:
The implementation of the TV allows to adapt the vehicle to a desired behaviour in

terms of understeering or oversteering response tendency together with the ability to adapt this behaviour with the driver desires and improve his/her feelings while driving.

- Energy management:

The tuning of TD in terms of priority objectives allows to reduce the consumption of energy.

- Performance improvement:

The implementation of the TV improves quite considerably the ability to work over more demanding driving requests, as it handles higher yaw rate references in a more suitable way than a vehicle without this technology. This benefit also leads to time per lap minimization, which is quite important for the purposes of the team.

- Tire ware management:

The implementation of TV allows to work over optimal conditions of the tire, reducing the ware of its rubber, which is suitable for reducing degradation (leading also to less sets of tires needed).

Further Work

- The current project of the team of developing a vehicle with multiple electrical machines has a short background of two seasons. For that reason, a possible improvement that can be done is to get more data of the vehicle and increase the accuracy of the results obtained by data analysis to complement the actual information available. For example, a crucial section to be improved is the tire logged information, which is quite difficult to be analyzed, reason that justifies why a simple circle of friction, and not a more complex one, has been used throughout this project.
- For further tests, other kind of controllers that could improve the results when working with state-space equations may be designed. Some considered suitable options could be H_∞ techniques or Model Predictive Control (MPC). So far, they have not been considered as options to be designed because of the computational power they require compared to the one needed for a PID controller type, apart from the previously mentioned desire to simplify the yaw rate controller.
- The inclusion of regenerative braking inside the algorithm to allow different braking torque on each motors to improve braking maneuvers. To do so, more data about regenerative energy management is necessary together with the design of an algorithm that properly mixes mechanical and regenerative braking.
- The implementation of the designed control inside the main ECU of the CAT13e, an ETAS ES910 module. Together with that, analyze the real results of the algorithm running inside ECU of the CAT13e.

Bibliography

- [Mil, 1994] (1994). In Milliken, W. F. and L. Milliken, D., editors, *Race Car Vehicle Dynamics*, page 918. SAE International, Warrendale, Pa. (USA).
- [Rac, 2014] (2014). In Steward, D., editor, *Race Car Design*, page 288. Palgrave Macmillan.
- [Han, 2015] (2015). Symbols. In Abe, M., editor, *Vehicle Handling Dynamics (Second Edition)*. Butterworth-Heinemann.
- [Anton Stoop, 2014] Anton Stoop, D. (2014). Design and implementation of torque vectoring for the forze racing car. Master's thesis, Mechanical, Maritime and Materials Engineering, TU Delft.
- [Antunes et al., 2019] Antunes, J., Antunes, A., Outeiro, P., Cardeira, C., and Oliveira, P. (2019). Testing of a torque vectoring controller for a formula student prototype. *Robotics and Autonomous Systems*, 113:56 – 62.
- [Blázquez Romañá, 2020] Blázquez Romañá, A. (2020). Analysis and design of a lateral force estimator for a formula student vehicle. Treball final de grau, UPC, Escola Tècnica Superior d'Enginyeria Industrial de Barcelona.
- [Doumiati et al., 2010] Doumiati, M., Sename, O., Martínez Molina, J., Dugard, L., and Poussot-Vassal, C. (2010). Gain-scheduled lpv/h controller based on direct yaw moment and active steering for vehicle handling improvements. *CDC 2010*.
- [Gang Liu et al., 2013] Gang Liu, Hongbin Ren, Sizhong Chen, and Wenzhu Wang (2013). The 3-dof bicycle model with the simplified piecewise linear tire model. In *Proceedings 2013 International Conference on Mechatronic Sciences, Electric Engineering and Computer (MEC)*, pages 3530–3534.
- [Karl Johan Åström, 2008] Karl Johan Åström, B. W. (2008). Adaptative control (second edition). Courier Corporation.
- [Kevin Ghezzi, 2017] Kevin Ghezzi, M. (2017). Control of a four in-wheel motor drive electric vehicle. Treball final de grau, UPC, Escola Tècnica Superior d'Enginyeria Industrial de Barcelona.
- [Lutsey and Hall, 2018] Lutsey, N. and Hall, D. (2018). Effects of battery manufacturing on electric vehicle life-cycle greenhouse gas emissions.

- [Marti Rubio, 2016] Marti Rubio, O. (2016). Lpv control of an autonomous vehicle. Master's thesis, Universitat Politècnica de Catalunya.
- [Mikle and Bat'a, 2019] Mikle, D. and Bat'a, M. (2019). Torque vectoring for an electric all-wheel drive vehicle. *IFAC-PapersOnLine*, 52(27):163 – 169. 16th IFAC Conference on Programmable Devices and Embedded Systems PDES 2019.
- [Pacejka, 2008] Pacejka, H. B. (2008). Tire and vehicle dynamics (3rd edition). page 672. Butterworth-Heinemann.
- [Rotondo et al., 2013] Rotondo, D., Nejjari, F., and Puig, V. (2013). Quasi-lpv modeling, identification and control of a twin rotor mimo system. *Control Engineering Practice*, 21(6):829 – 846.
- [Segers, 2008] Segers, J. (2008). Analysis techniques for racecar data acquisition, second edition. page 534. SAE International.
- [Shamma, 1988] Shamma, J. S. (1988). Analysis and design of gain scheduled control systems.
- [Smith, 1997] Smith, S. W. (1997). *The Scientist and Engineer's Guide to Digital Signal Processing*. California Technical Publishing, USA.
- [Trunas Bruguera, 2019] Trunas Bruguera, F. (2019). Disseny i implementació d'un algoritme de *torque vectoring* per un vehicle formula student. Treball final de grau, UPC, Escola Tècnica Superior d'Enginyeria Industrial de Barcelona.
- [Velazquez Alcantar and Assadian, 2019] Velazquez Alcantar, J. and Assadian, F. (2019). Vehicle dynamics control of an electric-all-wheel-drive hybrid electric vehicle using tyre force optimisation and allocation. *Vehicle System Dynamics*, pages 1–27.